Collisional relaxation of a strongly magnetized two-species pure ion plasma

Chi Yung Chim, Thomas M. O'Neil, and Daniel H. Dubin
Department of Physics, University of California at San Diego, La Jolla, California 92093, USA

(Received 17 February 2014; accepted 31 March 2014; published online 16 April 2014)

The collisional relaxation of a strongly magnetized pure ion plasma that is composed of two species with slightly different masses is discussed. We have in mind two isotopes of the same singly ionized atom. Parameters are assumed to be ordered as $\Omega_1, \Omega_2 \gg |\Omega_1 - \Omega_2| \gg \bar{v}_{ij}/\bar{b}$ and $\bar{v}_{\perp j}/\Omega_j \ll \bar{b}$, where Ω_1 and Ω_2 are two cyclotron frequencies, $\bar{v}_{ij} = \sqrt{T_\parallel/\mu_{ij}}$ is the relative parallel thermal velocity characterizing collisions between particles of species i and j, and $\bar{b} = 2e^2/T_\parallel$ is the classical distance of closest approach for such collisions, and $\bar{v}_{\perp j}/\Omega_j = \sqrt{2T_{\perp j}/m_j}/\Omega_j$ is the characteristic cyclotron radius for particles of species j. Here, μ_{ij} is the reduced mass for the two particles, and $T_\parallel$ and $T_{\perp j}$ are temperatures that characterize velocity components parallel and perpendicular to the magnetic field. For this ordering, the total cyclotron action for the two species, $\mathcal{I}_1 = \sum_{i\in 1} m_1 v_{\perp i}^2/(2\Omega_1)$ and $\mathcal{I}_2 = \sum_{i\in 2} m_2 v_{\perp i}^2/(2\Omega_2)$ are adiabatic invariants that constrain the collisional dynamics. On the timescale of a few collisions, entropy is maximized subject to the constancy of the total Hamiltonian H and the two actions $\mathcal{I}_1$ and $\mathcal{I}_2$, yielding a modified Gibbs distribution of the form $\exp[-H/T_\parallel - \alpha_1\mathcal{I}_1 - \alpha_2\mathcal{I}_2]$. Here, the α_j's are related to $T_\parallel$ and $T_{\perp j}$ through $T_{\perp j} = (1/T_\parallel + \alpha_j/\Omega_j)^{-1}$. Collisional relaxation to the usual Gibbs distribution, $\exp[-H/T_\parallel]$, takes place on two timescales. On a timescale longer than the collisional timescale by a factor of $(\bar{b}^2\Omega_1^2/\bar{v}_{11}^2)\exp\{5[3\pi(\bar{b}|\Omega_1 - \Omega_2|/\bar{v}_{12})]^{2/5}/6\}$, the two species share action so that α_1 and α_2 relax to a common value α. On an even longer timescale, longer than the collisional timescale by a factor of the order $\exp\{5[3\pi(\bar{b}\Omega_1/\bar{v}_{11})]^{2/5}/6\}$, the total action ceases to be a good constant of the motion and α relaxes to zero. © *2014 AIP Publishing LLC*. [http://dx.doi.org/10.1063/1.4871490]

I. INTRODUCTION

There is good agreement between theory and experiment for the collisional relaxation of strongly magnetized single species plasmas.[1–5] The relaxation is novel because the collisional dynamics is constrained by adiabatic invariants associated with the cyclotron motion. Here, we extend the theory to the case of a two-species plasma, where the charges of the two species are the same ($e_1 = e_2$) and the masses differ only slightly (i.e., $|m_1 - m_2| \ll m_1, m_2$). We have in mind a pure ion plasma that is composed of two isotopes. Such isotopically impure ion plasmas are often used in experiments.[6,7]

In Sec. II, we begin with an analysis of a collision between two isotopically different ions that move in the uniform magnetic field $\mathbf{B} = B\hat{z}$. For sufficiently strong magnetic field, the collision looks very different from Rutherford scattering; the two ions approach and move away from one another in tight helical orbits that follow magnetic field lines.

We will find that the sum of the cyclotron actions for the two ions, $I_1 + I_2 = m_1 v_{\perp 1}^2/(2\Omega_1) + m_2 v_{\perp 2}^2/(2\Omega_2)$, is an adiabatic invariant that is nearly conserved in the collision. Here, $m_j v_{\perp j}^2/2$ and $\Omega_j = eB/(m_j c)$ are the cyclotron kinetic energy and cyclotron frequency for the two ions ($j = 1,2$). More specifically, the change in the total action is of order $\Delta(I_1 + I_2) \sim \exp[-\Omega_c\tau]$, where $\Omega_1 \simeq \Omega_2 \equiv \Omega_c$ and τ is a time that characterizes the duration of the collision. The time is shortest, and the change $\Delta(I_1 + I_2)$ largest, for nearly head-on collisions, where $\tau \simeq (\pi/2)(b/v_\parallel)$. Here, $v_\parallel$ is the initial relative velocity of the ions parallel to the magnetic field, $b = 2e^2/(\mu v_\parallel^2)$ is the minimum separation between the ions allowed on energetic grounds, and $\mu \equiv m_1 m_2/(m_1 + m_2)$ is the reduced mass. This estimate of τ uses guiding center drift dynamics as a zeroth order approximation to the orbits and so assumes that the cyclotron radii for the two ions are small compared to the ion separation [i.e., $v_{\perp j}/\Omega_j \ll b$]. For sufficiently large B, the product $\Omega_c\tau = (\pi/2)(\Omega_c b/v_\parallel)$ is large compared to unity and the change $\Delta(I_1 + I_2) \sim \exp[-(\pi/2)(\Omega_c b/v_\parallel)]$ is exponentially small.

The same analysis shows that the change in the individual actions is of order $\Delta I_1 \simeq -\Delta I_2 \sim \exp[-|\Omega_1 - \Omega_2|\tau]$, which also is exponentially small if $|\Omega_1 - \Omega_2|[\pi b/(2v_\parallel)]$ is large. By assumption, the ion masses, and therefore the ion cyclotron frequencies, differ only slightly, so we have the ordering $\Omega_1, \Omega_2 \gg |\Omega_1 - \Omega_2| \gg v_\parallel/b$, which implies the conclusion

$$I_1, I_2 \gg |\Delta I_1| \simeq |\Delta I_2| \gg |\Delta(I_1 + I_2)|. \tag{1}$$

The individual actions are well conserved, and the sum of the two actions is conserved even better.

In Sec. III, we determine how these adiabatic invariants constrain the collisional relaxation of a strongly magnetized plasma composed of such ions. We say that the plasma is strongly magnetized when

 © 2014 AIP Publishing LLC

This article is copyrighted as indicated in the article. Reuse of AIP content is subject to the terms at: http://scitation.aip.org/termsconditions. Downloaded to IP: 132.239.69.167 On: Wed, 18 Mar 2015 17:53:47

$$\bar{b} \gg \frac{\bar{v}_{\perp,jk}}{\Omega_j} \quad \text{and} \quad |\Omega_1 - \Omega_2| \gg \frac{\bar{v}_{jk}}{\bar{b}}, \tag{2}$$

where $\bar{v}_{ij} = \sqrt{T_\parallel/\mu_{ij}}$ is the relative parallel thermal velocity, $\bar{b} = 2e^2/(\mu_{jk}\bar{v}_{jk}^2) = 2e^2/T_\parallel$ is the distance of closest approach, $\bar{v}_{\perp j} = \sqrt{2T_{\perp j}/m_j}$ is the perpendicular thermal velocity for species j, and μ_{jk} is the reduced mass of two interacting particles from species j and k. As we will see, the temperatures $T_\parallel$, $T_{\perp 1}$, and $T_{\perp 2}$ need not be equal during the evolution to thermal equilibrium. The condition $\Omega_1, \Omega_2 \gg |\Omega_1 - \Omega_2|$ plus inequalities (2) imply that all collisions between unlike ions are in the strongly magnetized parameter regime.

Note that this definition of strong magnetization is more restrictive than that used previously for the case of single-species plasmas.[3,4] The requirement $|\Omega_1 - \Omega_2| \gg \bar{v}_{jk}/\bar{b}$ has replaced the less restrictive requirement $\Omega_1, \Omega_2 \gg \bar{v}_{jk}/\bar{b}$.

As a first step in determining the influence of the adiabatic invariants on the evolution, we note that the difference between the cyclotron frequencies of like ions is zero, so the change in the individual actions is not exponentially small. Of course, the change in the sum of the two actions for the like ions is exponentially small.

Thus, on the timescale of a few collisions, one expects that like ions will interchange cyclotron action with each other, but not with unlike ions. On this timescale, the total cyclotron action of species 1 (i.e., $\mathcal{I}_1 = \sum_{j=1}^{N_1} I_{1j}$) and the total cyclotron action of species 2 (i.e., $\mathcal{I}_2 = \sum_{j=1}^{N_2} I_{2j}$) along with the total Hamiltonian $\mathcal{H}$ are constants of the motion, and a modified Gibbs distribution, $\exp[-\mathcal{H}/T_\parallel - \alpha_1\mathcal{I}_1 - \alpha_2\mathcal{I}_2]$ is established.[8] Here $T_\parallel$, α_1 and α_2 are thermodynamic variables. From the velocity dependence in $\mathcal{H}$, $\mathcal{I}_1$ and $\mathcal{I}_2$, one can see that $T_\parallel$ is the temperature that characterizes velocity components parallel to the magnetic field and that $T_{\perp 1} = [1/T_\parallel + \alpha_1/\Omega_1]^{-1}$ and $T_{\perp 2} = [1/T_\parallel + \alpha_2/\Omega_2]^{-1}$ are the temperatures that characterize the perpendicular velocity components for species 1 and 2.

Inequalities (2) imply that on a longer timescale particles of the two species interchange action with each other conserving the sum $\mathcal{I}_1 + \mathcal{I}_2$. On this timescale, the variables α_1 and α_2 evolve to a common value, yielding the distribution $\exp[-\mathcal{H}/T_\parallel - \alpha(\mathcal{I}_1 + \mathcal{I}_2)]$, where α is that common value. On a still longer timescale, $\mathcal{I}_1 + \mathcal{I}_2$ is not conserved, and α evolves to zero, yielding the usual Gibbs distribution $\exp[-\mathcal{H}/T_\parallel]$.

The purpose of this paper is to calculate the rate at which α_1 and α_2 evolve to the common value α and the much slower rate at which α evolves to zero. We will find that $\alpha_1 - \alpha_2$ satisfies the equation,

$$\frac{d}{dt}(\alpha_1 - \alpha_2) = -\nu_a(\alpha_1 - \alpha_2) \tag{3}$$

and that α satisfies the equation

$$\frac{d}{dt}\alpha = -\nu_b\alpha, \tag{4}$$

where ν_a is of the order $\mathcal{O}[n\bar{b}_0^2\bar{v}_{11,0}\Lambda_2(\bar{b}|\Omega_1 - \Omega_2|/\bar{v}_{12})(\bar{v}_{11}/(\bar{b}\Omega_1))^2]$ and ν_b is of the order $\mathcal{O}[n\bar{b}_0^2\bar{v}_{11,0}\Lambda_1(\bar{b}\Omega_1/\bar{v}_{11})]$, and subscript 0 refers to initial values before equilibration. $\Lambda_1(\bar{\kappa})$ and $\Lambda_2(\bar{\kappa})$ decrease exponentially with increasing $\bar{\kappa}$. In the limit of $\bar{\kappa} \gg 1$, $\Lambda_1(\bar{\kappa})$ and $\Lambda_2(\bar{\kappa})$ are approximated by the asymptotic expressions,

$$\Lambda_1(\bar{\kappa}) \simeq 3.10\bar{\kappa}^{-7/15}e^{-5(3\pi\bar{\kappa})^{2/5}/6}, \tag{5}$$

$$\Lambda_2(\bar{\kappa}) \simeq 3.87\bar{\kappa}^{13/15}e^{-5(3\pi\bar{\kappa})^{2/5}/6}. \tag{6}$$

In $\Lambda_1(\bar{\kappa})$, $\bar{\kappa}$ is the magnetization $\bar{\kappa}_{ij} = \bar{b}\Omega_i/\bar{v}_{ij}$, whereas in $\Lambda_2(\bar{\kappa})$, $\bar{\kappa}$ is the magnetization difference $|\bar{\kappa}_{12} - \bar{\kappa}_{21}|$, when Λ_1 and Λ_2 are used to describe the equipartition rates.

II. TWO-PARTICLE COLLISION

In this section, we consider the isolated collision of two ions that have equal charges ($e_1 = e_2 \equiv e$), slightly different masses ($|m_1 - m_2| \ll m_1, m_2$), and move in the uniform magnetic field $\mathbf{B} = B\hat{z}$. The Hamiltonian for the two interacting charges can be written as

$$H = \sum_{k=1}^{2}\left[\frac{p_{zk}^2}{2m_k} + \frac{p_{xk}^2}{2m_k} + \frac{(p_{yk} - eBx/c)^2}{2m_k}\right] + \frac{e^2}{[(x_1 - x_2)^2 + (y_1 - y_2)^2 + (z_1 - z_2)^2]^{1/2}}, \tag{7}$$

where we have used the vector potential $\mathbf{A} = Bx\hat{y}$, and the quantities (x_k,p_{xk}), (y_k,p_{yk}), (z_k,p_{zk}) are canonically conjugate coordinates and momenta.[9]

We assume that the magnetic field strength and initial velocities satisfy the conditions for strong magnetization as defined in Sec. I (i.e., $v_{\perp j}/\Omega_j \ll b$ and $|\Omega_1 - \Omega_2| \gg v_\parallel/b$). In this limit, the following transformation[10] is useful:

$$Y_k = y_k - \frac{c}{eB}p_{xk}, \tag{8}$$

$$X_k = \frac{c}{eB}p_{yk}, \tag{9}$$

$$\psi_k = -\tan^{-1}\left(\frac{y_k - Y_k}{x_k - X_k}\right), \tag{10}$$

$$I_k = \frac{p_{xk}^2 + (p_{yk} - eBx_k/c)^2}{2m_k\Omega_k}. \tag{11}$$

One can check that (z_k,p_{zk}), $(Y_k, P_{Y_k} \equiv \frac{eB}{c}X_k)$ and (ψ_k, I_k) satisfy the usual Poisson brackets required of canonically conjugate coordinates and momenta, i.e., $\{q_i, p_j\} = \delta_{ij}$. Here (X_k,Y_k) are the coordinates of the guiding center for the k-th particle, and (ψ_k, I_k) are the gyro-angle and cyclotron action for the k-th particle. In terms of these new canonical variables, the Hamiltonian takes the form

$$H = \sum_{k=1}^{2}\left(\frac{p_{zk}^2}{2m_k} + \Omega_k I_k\right) + \frac{e^2}{|\mathbf{r}_1 - \mathbf{r}_2|}, \tag{12}$$

where

$$|\mathbf{r}_1 - \mathbf{r}_2|^2 = (z_1 - z_2)^2 + (X_1 + \rho_1\cos\psi_1 - X_2 - \rho_2\cos\psi_2)^2 + (Y_1 - \rho_1\sin\psi_1 - Y_2 + \rho_2\sin\psi_2)^2. \tag{13}$$

This article is copyrighted as indicated in the article. Reuse of AIP content is subject to the terms at: http://scitation.aip.org/termsconditions. Downloaded to IP: 132.239.69.167 On: Wed, 18 Mar 2015 17:53:47

Here, $\rho_k = \sqrt{2I_k/(m_k\Omega_k)}$ is the cyclotron radius of the k-th particle.

Since $|\mathbf{r}_1 - \mathbf{r}_2|$ is periodic in ψ_1 and ψ_2, the Hamiltonian can be written in the form

$$H = \sum_{k=1}^{2}\left(\frac{p_{zk}^2}{2m_k} + \Omega_k I_k\right) + \sum_{\mu,\nu} g_{\mu\nu} e^{i(\mu\psi_1+\nu\psi_2)}, \tag{14}$$

where $g_{\mu\nu} = g_{\mu\nu}(I_1, I_2, z_1 - z_2, X_1 - X_2, Y_1 - Y_2)$, and μ and ν run over all integer values from $-\infty$ to $+\infty$.

We will find it instructive to calculate the change over the course of the collision in the sum and difference of the cyclotron actions, $\Delta(I_1 + I_2)$ and $\Delta(I_1 - I_2)$. Hamilton's equations yield the time derivatives

$$\frac{d}{dt}(I_1 + I_2) = -\left(\frac{\partial}{\partial\psi_1} + \frac{\partial}{\partial\psi_2}\right)H = -\sum_{\mu\nu} i(\mu+\nu) g_{\mu\nu} e^{i(\mu\psi_1+\nu\psi_2)} \tag{15}$$

and

$$\frac{d}{dt}(I_1 - I_2) = -\left(\frac{\partial}{\partial\psi_1} - \frac{\partial}{\partial\psi_2}\right)H = -\sum_{\mu\nu} i(\mu-\nu) g_{\mu\nu} e^{i(\mu\psi_1+\nu\psi_2)}. \tag{16}$$

For strong magnetization, one expects guiding center drift theory to provide a good zeroth order approximation to the particle orbits. Moreover, the guiding center variables are slowly varying in time compared to the rapidly varying gyro-angles ψ_1 and ψ_2. In this approximation, the arguments of $g_{\mu\nu} = g_{\mu\nu}(I_1, I_2, z_1 - z_2, X_1 - X_2, Y_1 - Y_2)$ are slowly varying and the exponentials $e^{i(\mu\psi_1+\nu\psi_2)}$ are rapidly oscillating, and the time integral of such a product phase mixes to a small value. We will find that the value is exponentially small in the ratio of the rapid to the slow timescales.

At this point, we can anticipate the main result of the calculation. The smallest frequency for the exponentials is $|\Omega_1 - \Omega_2|$, corresponding to the choice $\mu = -\nu = \pm 1$. Since the coefficient for this term vanishes identically in Eq. (15) but not in Eq. (16), the change $|\Delta(I_1 + I_2)|$ is much smaller than the change $|\Delta(I_1 - I_2)|$. Equivalently, one may say that the total action is conserved to much better accuracy than either of the two actions independently, i.e., $|\Delta(I_1 + I_2)| \ll |\Delta I_1|, |\Delta I_2|$.

The guiding center Hamiltonian[11,12] is obtained simply by setting $\rho_1 = \rho_2 = 0$ in Eq. (13), yielding

$$H_{GC} = \sum_{k=1}^{2}\left(\frac{p_{zk}^2}{2m_k} + \Omega_k I_k\right) + \frac{e^2}{[(z_1 - z_2)^2 + (X_1 - X_2)^2 + (Y_1 - Y_2)^2]^{1/2}}, \tag{17}$$

where $P_{Y_k} = \frac{c}{eB} X_k$. Making the canonical transformation to center-of-mass and relative coordinates,

$$z = z_1 - z_2, \tag{18}$$

$$Z = \frac{m_1 z_1 + m_2 z_2}{m_1 + m_2}, \tag{19}$$

$$p_z = \frac{m_2 p_{z1} - m_1 p_{z2}}{m_1 + m_2}, \tag{20}$$

$$P_Z = p_{z1} + p_{z2} \tag{21}$$

yields the Hamiltonian

$$H_{GC} = \frac{P_Z^2}{2M} + \frac{p_z^2}{2\mu} + I_1\Omega_1 + I_2\Omega_2 + \frac{e^2}{[(z_1 - z_2)^2 + (X_1 - X_2)^2 + (Y_1 - Y_2)^2]^{1/2}}, \tag{22}$$

where $M = m_1 + m_2$ and $\mu = m_1 m_2/(m_1 + m_2)$.

Thus, with guiding center dynamics, the quantities H_{GC}, P_Z, I_1, I_2, and $(X_1 - X_2)^2 + (Y_1 - Y_2)^2 \equiv |\Delta\mathbf{R}_\perp|^2$ are constants of the motion, and the relative coordinate $z(t)$ is governed by the equation

$$\frac{\mu\dot{z}^2(t)}{2} + \frac{e^2}{(|\Delta\mathbf{R}_\perp|^2 + z^2(t))^{1/2}} = \frac{\mu v_\parallel^2}{2}, \tag{23}$$

where $v_\parallel \equiv \dot{z}(t = -\infty)$ is the initial relative velocity. From this equation, one sees that the minimum allowed separation between the guiding centers is given by $b = \sqrt{|\Delta\mathbf{R}_\perp|^2 + z^2|_{\min}} = 2e^2/(\mu v_\parallel^2)$. We choose $t = 0$ so that $z^2(t)$ is an even function of t. For the case where $|\Delta\mathbf{R}_\perp| < b$, there is no reflection and we choose $z(0) = 0$, and for the case where $|\Delta\mathbf{R}_\perp| > b$, we choose $t = 0$ to be at the point of reflection, that is, $z^2(0) = b^2 - (\Delta\mathbf{R}_\perp^2)$.

In the guiding center drift approximation, the most rapidly varying variable in the argument of $g_{\mu\nu}(I_1, I_2, z_1 - z_2, X_1 - X_2, Y_1 - Y_2)$ is the relative coordinate $z(t) = z_1(t) - z_2(t)$, and the timescale associated with this variation is of order $b/v_\parallel$ or larger. By comparison, the timescale for the oscillatory variation of the exponential $\exp(i\mu\psi_1 + i\nu\psi_2)$ is $|\mu\Omega_1 + \nu\Omega_2|^{-1} < |\Omega_1 - \Omega_2|^{-1}$. Thus, the strong magnetization ordering $v_\parallel/b \ll |\Omega_1 - \Omega_2| \ll \Omega_1, \Omega_2$ is simply a statement of the needed separation of timescales.

We Taylor expand $g_{\mu\nu}$ in powers of $\rho_k/\sqrt{|\Delta\mathbf{R}_\perp|^2 + z^2} \le \rho_k/b \ll 1$. As one would expect, each term in the expansion of $g_{\mu\nu}$ is of order $(\rho/b)^{|\mu|+|\nu|}$, and for simplicity we retain only the lowest order term. An equivalent way to do so is to expand H in powers of ρ_k and collect terms of the right Fourier dependence $\exp(i\mu\psi_1 + i\nu\psi_2)$, so as to obtain the Taylor-approximated $g_{\mu\nu}$. Expressions of $g_{\mu\nu}$ that are used in the calculation are the following:

$$g_{10} = -\frac{e^{i(\Omega_1 t+\phi_1)}}{2}\frac{e^2 v_{\perp 1}/\Omega_1}{|\Delta\mathbf{R}_\perp|^2 + z^2} = g_{-1,0}^*, \tag{24}$$

$$g_{01} = \frac{e^{i(\Omega_2 t+\phi_2)}}{2}\frac{e^2 v_{\perp 2}/\Omega_2}{|\Delta\mathbf{R}_\perp|^2 + z^2} = g_{0,-1}^*, \tag{25}$$

This article is copyrighted as indicated in the article. Reuse of AIP content is subject to the terms at: http://scitation.aip.org/termsconditions. Downloaded to IP: 132.239.69.167 On: Wed, 18 Mar 2015 17:53:47

$$g_{1,-1} = -\frac{e^{i(\Omega_1-\Omega_2)t+i(\phi_1-\phi_2)}}{2}\frac{e^2}{(|\Delta\mathbf{R}|^2+z^2)^{3/2}} \times\left(1-\frac{3|\Delta\mathbf{R}_\perp|^2}{2(|\Delta\mathbf{R}_\perp|^2+z^2)}\right)\frac{v_{\perp1}v_{\perp2}}{\Omega_1\Omega_2} = g^*_{-1,1}, \quad (26)$$

where $v_{\perp k} = \rho_k\Omega_k$ is the cyclotron velocity, $\phi_k = \psi_k(t=0)$ is the gyroangle at $t=0$, and as mentioned earlier we choose $t=0$ so that $z^2(t)$ is an even function of time. Also we note that $|g_{10}|$ and $|g_{01}|$ are of the order $\rho_k \propto \Omega_k^{-1} \propto B^{-1}$, but $|g_{1,-1}|$ is of the order $\rho_k^2 \propto \Omega_k^{-2} \propto B^{-2}$.

Since the time integrals $\int_{-\infty}^{\infty} dt g_{\mu\nu}\exp(i\mu\psi_1 + i\nu\psi_2)$ turn out to be exponentially small in the ratio of the slow to rapid timescales, we need only to retain the lowest frequency terms in the sum over μ and ν. Specifically, we retain the terms with frequencies $|\Omega_1-\Omega_2|$, Ω_1, and Ω_2, using Eqs. (24)–(26) to obtain the results

$$\Delta(I_1-I_2) = -\int_{-\infty}^{\infty} e^2\frac{v_{\perp2}}{\Omega_2}\sin\phi_2\frac{|\Delta\mathbf{R}_\perp|}{(|\Delta\mathbf{R}_\perp|^2+z^2)^{3/2}}\cos(\Omega_2 t)dt - \int_{-\infty}^{\infty} e^2\frac{v_{\perp1}}{\Omega_1}\sin\phi_1\frac{|\Delta\mathbf{R}_\perp|}{(|\Delta\mathbf{R}_\perp|^2+z^2)^{3/2}}\cos(\Omega_1 t)dt + \int_{-\infty}^{\infty}\frac{e^2v_{\perp1}v_{\perp2}}{(|\Delta\mathbf{R}_\perp|^2+z^2)^{3/2}}\frac{2}{\Omega_1\Omega_2}\cos[(\Omega_1-\Omega_2)t]\sin(\phi_1-\phi_2)\left(1-\frac{3|\Delta\mathbf{R}_\perp|^2}{2(|\Delta\mathbf{R}_\perp|^2+z^2)}\right)dt, \quad (27)$$

and

$$\Delta(I_1+I_2) = \int_{-\infty}^{\infty} e^2\frac{v_{\perp2}}{\Omega_2}\sin\phi_2\frac{|\Delta\mathbf{R}_\perp|}{(|\Delta\mathbf{R}_\perp|^2+z^2)^{3/2}}\cos(\Omega_2 t)dt - \int_{-\infty}^{\infty} e^2\frac{v_{\perp1}}{\Omega_1}\sin\phi_1\frac{|\Delta\mathbf{R}_\perp|}{(|\Delta\mathbf{R}_\perp|^2+z^2)^{3/2}}\cos(\Omega_1 t)dt. \quad (28)$$

The integrals carrying $\cos(\Omega_i t)$ are proportional to

$$f_1(\kappa_i,\eta) = \int_{-\infty}^{\infty}\frac{d\xi\cos(\kappa_i\xi)}{(\eta^2+\zeta^2(\xi))^{3/2}}, \quad (29)$$

while the integral carrying $\cos[(\Omega_1-\Omega_2)t]$ is proportional to

$$f_2(\kappa_1-\kappa_2,\eta) = \int_{-\infty}^{\infty}\frac{d\xi\cos[(\kappa_1-\kappa_2)\xi]}{(\eta^2+\zeta^2(\xi))^{3/2}}\left(1-\frac{3\eta^2}{2[\eta^2+\zeta^2(\xi)]}\right), \quad (30)$$

where $\xi = v_\parallel t/b$, $\kappa_i = b\Omega_i/v_\parallel$, $\eta = |\Delta\mathbf{R}_\perp|/b$ and $\zeta = z/b$. In terms of these variables, differential equation (23) takes the form

$$\left(\frac{d\zeta}{d\xi}\right)^2 + \frac{1}{\sqrt{\eta^2+\zeta^2(\xi)}} = 1, \quad (31)$$

where $\zeta^2(0) = \max(0, 1-\eta^2)$. In Sec. III, we will need the results

$$\Delta(I_1+I_2) = -\frac{e^2}{b\Omega_1}\left(\frac{v_{\perp1}}{v_\parallel}\sin\phi_1\right)\eta f_1(\kappa_1,\eta) + \frac{e^2}{b\Omega_2}\left(\frac{v_{\perp2}}{v_\parallel}\sin\phi_2\right)\eta f_1(\kappa_2,\eta), \quad (32)$$

$$\Delta I_1 = -\frac{e^2}{b\Omega_1}\left(\frac{v_{\perp1}}{v_\parallel}\sin\phi_1\right)\eta f_1(\kappa_1,\eta) + \frac{e^2}{b\Omega_1\Omega_2}\frac{v_{\perp1}v_{\perp2}}{v_\parallel b}f_2(\kappa_1-\kappa_2,\eta)\sin(\phi_1-\phi_2), \quad (33)$$

$$\Delta I_2 = \frac{e^2}{b\Omega_2}\left(\frac{v_{\perp2}}{v_\parallel}\sin\phi_2\right)\eta f_1(\kappa_2,\eta) + \frac{e^2}{b\Omega_1\Omega_2}\frac{v_{\perp1}v_{\perp2}}{v_\parallel b}f_2(\kappa_1-\kappa_2,\eta)\sin(\phi_2-\phi_1). \quad (34)$$

In the regime of strong magnetization (i.e., $1 \ll |\kappa_1-\kappa_2| \ll \kappa_1,\kappa_2$), the integrals f_1 and f_2 are exponentially small, since the integrands are the product of a rapidly oscillating cosine and a slowly varying function. The rapid oscillation makes a direct evaluation of such integrals difficult.

In Appendix, we analytically continue the integrals into the complex ξ-plane, making the exponentially small value of the integrals manifest in the integrands themselves. This facilitates numerical evaluation of the integrals and yields the asymptotic forms

$$f_1(\kappa_j,\eta) = h_1(\kappa_j,\eta)\exp[-g(\eta)\kappa_j], \quad (35)$$

$$f_2(|\kappa_1-\kappa_2|,\eta) = h_2(|\kappa_1-\kappa_2|,\eta)\exp[-g(\eta)|\kappa_1-\kappa_2|], \quad (36)$$

where

$$g(\eta) = \left|\int_1^\eta\frac{x^{3/2}dx}{\sqrt{(x-1)(\eta^2-x^2)}}\right| \quad (37)$$

is shown in Fig. 1. From the numerical evaluations, one can see that the quantities $h_j(\kappa,\eta)$ are neither exponentially small nor large. Also for $\eta=0$, one can show that $h_j(\kappa,0) = h_2(\kappa,0) \simeq 8\pi\kappa/9$. In Sec. III, we will need the asymptotic forms only for small η. Fig. 2 shows a comparison of the numerical solution for $f_1(\kappa,0) = f_2(\kappa,0) \equiv f(\kappa)$ (solid curve) with the asymptotic solution (dashed curve).

As expected, the asymptotic forms are exponentially small in the ratio of the slow to fast timescales. For example, for f_1 the fast timescale is $\tau_f = \Omega_j^{-1}$ and the slow timescale is $\tau_s \simeq (\pi/2)(b/v_\parallel)$ for $\eta = |\mathbf{R}_\perp|/b < 1$ and $\tau_s \simeq |\mathbf{R}_\perp|/v_\parallel$ for $\eta > 1$. Note from Fig. 1 that $g(0) = \pi/2$ and that $g(\eta) \approx \eta$ for $\eta \gg 1$. For f_2, the only difference is that the fast timescale is $|\Omega_1-\Omega_2|^{-1}$.

This article is copyrighted as indicated in the article. Reuse of AIP content is subject to the terms at: http://scitation.aip.org/termsconditions. Downloaded to IP: 132.239.69.167 On: Wed, 18 Mar 2015 17:53:47

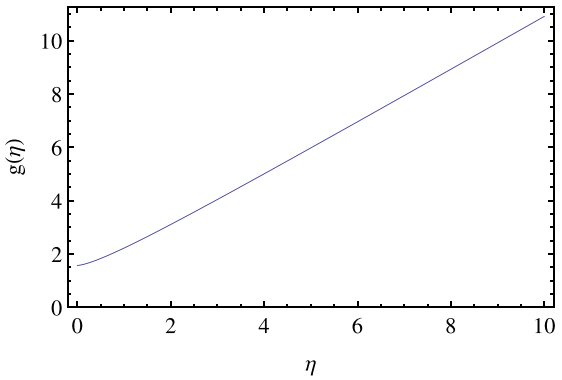

FIG. 1. Graph of $g(\eta)$.

For strong magnetization (i.e., $1 \ll |\kappa_1 - \kappa_2| \ll \kappa_1, \kappa_2$), the asymptotic forms verify the expected ordering for the changes in the actions (i.e., $|\Delta(I_1 + I_2)| \ll |\Delta I_1|, |\Delta I_2| \ll 1$).

As a check on the accuracy of Eqs. (32)–(34), we compare the predictions for $\Delta(I_1 - I_2)$ and $\Delta(I_1 + I_2)$ with results obtained by direction numerical integrations of the equations of motion for some sample collisions. For these comparisons, we choose $m_2 = m_1 + 0.1m_1$ and $v_{\perp 1} = v_{\perp 2} = 0.01v_\parallel$. The two particles are initially separated by the distance $d = 100b$ and given the intial relative velocity $v_z = v_\parallel \sqrt{1 - b/\sqrt{|\Delta \mathbf{R}|^2 + d^2}}$. The collision ends when the particles are again separated in the z-direction by the distance d. The motion is followed with a sixth-order Runge-Kutta algorithm,[13] using a timestep that is sufficiently small for the error in the total energy to be small compared to the change $\Delta(E_{\perp 1} + E_{\perp 2})$. The phase angles ϕ_j are varied to obtain the peak-to-peak variation in $\Delta(I_1 - I_2)$ and $\Delta(I_1 + I_2)$. The solid curves in Figs. 3 and 4 are the predictions of Eqs. (32)–(34), with numerical evaluation of integrals (29) and (30), for the scaled changes $\Delta(I_1 - I_2)/(m_1 v_{\perp 1}^2/\Omega_1)$ and $\Delta(I_1 + I_2)/(m_1 v_{\perp 1}^2/\Omega_1)$, respectively. The points result from integrating the particle equations of motion. For the collisions in these figures, η is near zero, and κ_2 is varied over a range of values. Of course, $\kappa_1 = 1.1\kappa_2$ and $|\kappa_2 - \kappa_1| = 0.1\kappa_2$. In Fig. 5, κ_1 is fixed at the value 21.0, and η is varied. We can see from the figures that our theory matches with the simulation results as long as magnetization is strong, i.e. $\kappa_1 \gg 1$. Particularly from Fig. 4, it is evident that the theory breaks down when κ_1 goes lower than around 2.

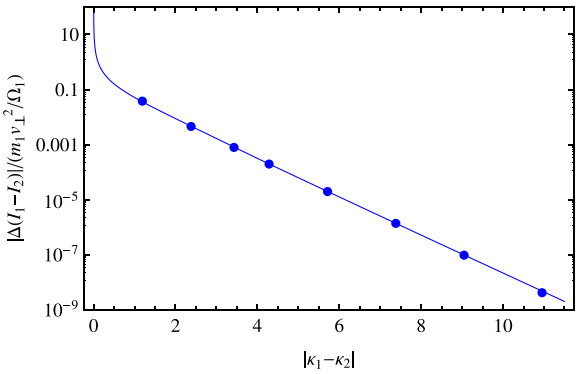

FIG. 3. Change in cyclotron action difference vs $|\kappa_1 - \kappa_2| = \kappa_1/11$. Here $v_{\perp 1} = v_{\perp 2} = 0.5v_\parallel$ and $m_2 = 1.1m_1$.

III. COLLISIONAL EVOLUTION OF A PLASMA

This section discusses the collisional evolution of a two species, strongly magnetized, pure ion plasma. Species 1 consists of N_1 singly ionized atoms of mass m_1 and species 2 of N_2 singly ionized atoms of mass m_2, where $|m_1 - m_2| \ll m_1, m_2$. For simplicity, the plasma is assumed to be uniform and immersed in a continuous neutralizing background charge. A laboratory realization of such a plasma is a thermal equilibrium, pure ion plasma that is confined in a Malmberg-Penning trap. Plasma rotation in the uniform axial magnetic field of the trap is equivalent to neutralization by a continuous background charge.

The plasma is assumed to be in the weakly correlated parameter regime, $e^2 n^{1/3}/T_\parallel \ll 1$, where n is the density.[14,15] The inequality can be written as $\bar{b} \ll n^{-1/3}$, so close collisions, which are primarily responsible for changes in the cyclotron actions, are well separated binary interactions of the kind considered in Sec. II. Furthermore, the plasma is assumed to satisfy the strong magnetization ordering in Eq. (2), so all collisions between unlike ions are of the kind considered in Sec. II.

To understand the final assumption, first recall from Eqs. (32)–(34) of the Sec. II that the change in actions during a collision depends sinusoidally on the initial gyroangles

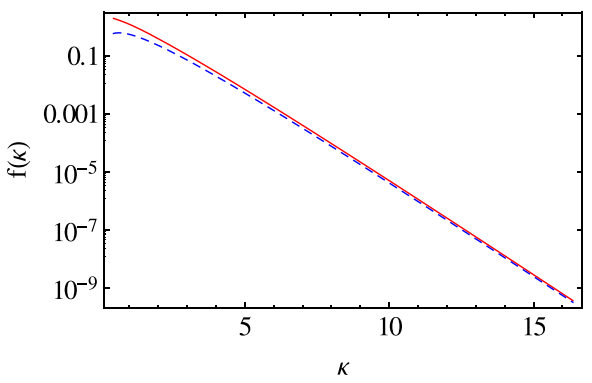

FIG. 2. Values of $f(\kappa)$. Solid line: numerical integration of $f(\kappa)$. Dashed line: asymptotic expression for large κ.

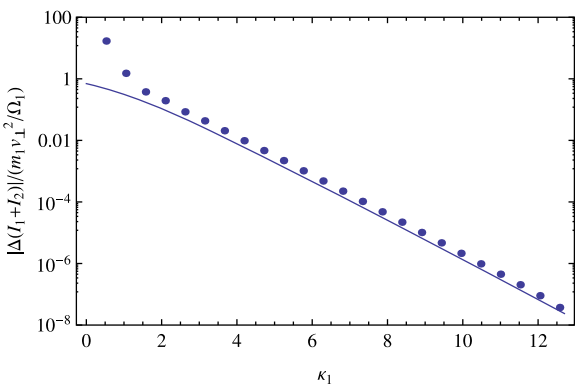

FIG. 4. Change in cyclotron action sum vs magnetization κ_1. Dots: simulation results. Line: values using numerical integration of $f_1(\kappa_1, \eta = 0)$.

This article is copyrighted as indicated in the article. Reuse of AIP content is subject to the terms at: http://scitation.aip.org/termsconditions. Downloaded to IP: 132.239.69.167 On: Wed, 18 Mar 2015 17:53:47

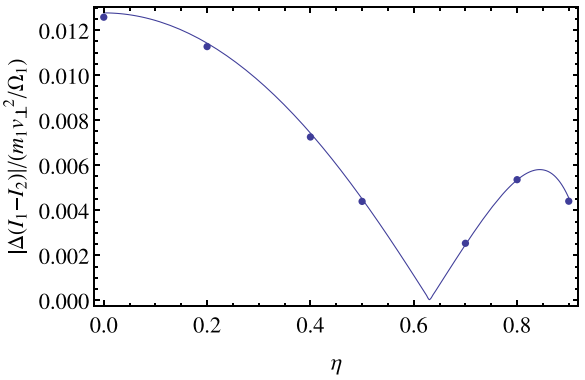

FIG. 5. Change in cyclotron action difference vs rescaled transverse separation η, for $\kappa_1 = 21$ and $|\kappa_1 - \kappa_2| = 1.9$. Dots: simulation results. Line: values using exact numerical integration of $f_2(|\kappa_1 - \kappa_2|, \eta)$.

$\phi_{kj} = \phi_{kj}(t = 0)$. The time between close collisions is much larger than a cyclotron period, so we assume that the particles enter each collision with random gyroangles.

Thus, the N-particle dynamics consists of many statistically independent, binary interactions of the kind considered in Sec. II. In this section, we simply establish a statistical framework to understand the cumulative effect of these collisions. The derivation follows an approach similar to the Green-Kubo relations.[16]

For a collision between unlike particles, we found in Sec. II that the changes in the individual actions are exponentially small, $|\Delta I_1| \simeq |\Delta I_2| \sim \mathcal{O}(\exp[-\pi|\kappa_1 - \kappa_2|/2])$, and that the change in the sum of the actions is even smaller $|\Delta(I_1 + I_2)| \sim \mathcal{O}(\exp[-\pi\kappa/2])$. However, for a collision between like particles, the change in the individual actions is not exponentially small since $\Omega_1 = \Omega_2$ and $\exp[-\pi/2|\kappa_1 - \kappa_2|] = 1$. Of course, the change in the sum of the actions is exponentially small since $\kappa = \kappa_1 \simeq \kappa_2 \gg 1$.

Thus, on the timescale of a few collisions, one expects the like particles to interchange action with each other nearly preserving the sums $\mathcal{I}_1 = \sum_{j=1}^{N_1} I(j_1)$ and $\mathcal{I}_2 = \sum_{j=2}^{N_2} I(j_2)$, where $I(j_k)$ is the action of the j-th particle of species k ($k = 1,2$). Maximizing entropy subject to the constancy of the total Hamiltonian $\mathcal{H}$ and the total actions $\mathcal{I}_1$ and $\mathcal{I}_2$ yields a modified Gibbs distribution of the form[8]

$$D_0 = \frac{1}{Z}\exp\left[-\frac{\mathcal{H}}{T_\parallel} - \alpha_1\mathcal{I}_1 - \alpha_2\mathcal{I}_2\right], \tag{38}$$

where Z and the thermodynamic variables $T_\parallel$, α_1 and α_2 are determined by the normalization $1 = \int d\Gamma D_0(\Gamma)$ and the expectation values

$$\langle\mathcal{I}_k\rangle = \int d\Gamma D_0(\Gamma)\mathcal{I}_k = \frac{N_k}{\alpha_k + \Omega_k/T_\parallel}, \tag{39}$$

$$\langle\mathcal{H}\rangle = \int d\Gamma D_0(\Gamma)\mathcal{H} = (N_1 + N_2)T_\parallel + \langle\mathcal{I}_1\rangle\Omega_1 + \langle\mathcal{I}_2\rangle\Omega_2 + \mathcal{U}_{\rm corr}. \tag{40}$$

Here, $d\Gamma$ is a volume element in the N-particle phase space ($N = N_1 + N_2$). The first three terms in the expression for $\langle\mathcal{H}\rangle$ are kinetic energy terms, whose form can be understood from the velocity dependence in $\mathcal{H}$ [i.e., $\sum_{j=1}^{N_1} m_1(v_{\parallel j}^2 + v_{\perp j}^2)/2 + \sum_{j=1}^{N_2} m_2(v_{\parallel j}^2 + v_{\perp j}^2)/2$] and in $\mathcal{I}_k$ [i.e., $\sum_{j=1}^{N_k} m_k v_{\perp j}^2/(2\Omega_k)$]. The last term, $\mathcal{U}_{\rm corr}$, is the correlation energy due to the interaction potentials in $\mathcal{H}$. For a weakly correlated and neutralized plasma, this latter term is small compared to the kinetic energy terms,[14] so we drop this term and use

$$\langle\mathcal{H}\rangle \simeq \frac{(N_1 + N_2)T_\parallel}{2} + \langle\mathcal{I}_1\rangle\Omega_1 + \langle\mathcal{I}_2\rangle\Omega_2. \tag{41}$$

Because the $\mathcal{I}_k$'s are not exact constants of the motion, the Liouville distribution, D, is not given exactly by D_0. We set $D = D_0 + D_1$, where D_1 is a small correction due to the time variation of the $\mathcal{I}_k$. Also, the thermodynamic variables, $T_\parallel$, α_1 and α_2 vary slowly in time, and the purpose of this section is to determine that variation.

To that end, we must evaluate the rates of change

$$\frac{d\langle\mathcal{I}_k\rangle}{dt} = \int d\Gamma\frac{\partial D}{\partial t}\mathcal{I}_k = \int d\Gamma D\{\mathcal{I}_k, \mathcal{H}\}, \tag{42}$$

$$\frac{d\langle\mathcal{H}\rangle}{dt} = \int d\Gamma\frac{\partial D}{\partial t}\mathcal{H} = \int d\Gamma D\{\mathcal{H}, \mathcal{H}\} = 0, \tag{43}$$

where $\{,\}$ is the Poisson bracket, and use has been made of the Liouville equation, $0 = \frac{dD}{dt} = \frac{\partial D}{\partial t} + \{D, \mathcal{H}\}$, and of integration by parts.

There is a subtle point in the evaluation of the Right Hand Side of Eq. (42). If one were to approximate D by D_0, the resulting integral would be zero

$$\int d\Gamma D_0\{\mathcal{I}_k, \mathcal{H}\} = \int d\Gamma\sum_{j=1}^{N_k}\left(-T_\parallel\frac{\partial D_0}{\partial\psi_{kj}}\right) = 0, \tag{44}$$

where ψ_{kj} is the gyroangle conjugate to I_{kj} and use has been made of the facts that the only dependence on ψ_{kj} is in $\mathcal{H}$ and that dependence is periodic. The non-zero contribution to the Right Hand Side of Eq. (42) comes exclusively from D_1, and to know D_1 one must solve the Liouville equation.

We suppose that at some time $t - \tau$, the correction D_1 is zero and let D_1 develop through the collisional dynamics. From the Liouville equation, $dD/dt = 0$, one finds that $D(t, \Gamma) = D_0[t - \tau, \Gamma'(\Gamma, -\tau)]$ where the phase point $\Gamma' = \Gamma'(\Gamma, t' - t)$ evolves to the phase point Γ as the time evolves from t' to t. In evaluating $D_0[t - \tau, \Gamma']$, we use $\mathcal{H}(\Gamma') = \mathcal{H}(\Gamma)$ and $\mathcal{I}_k(\Gamma') = \mathcal{I}_k(\Gamma) - \delta\mathcal{I}_k$, where

$$\delta\mathcal{I}_k = \int_{t-\tau}^{t} dt'\{\mathcal{I}_k, \mathcal{H}\}|_{\Gamma'(\Gamma, t'-t)}. \tag{45}$$

By hypothesis, $\mathcal{I}_k$ changes through a sequence of close collisions entered with randomly phased initial gyroangles. Thus, one can think of $\mathcal{I}_k(t)$ as a stochastic variable that suffers a sequence of many small and random changes. The correlation time for $\dot{\mathcal{I}}_k(t)$ is about the duration of a close collision, and the change in $\mathcal{I}_k(t)$ during that time is small.

This article is copyrighted as indicated in the article. Reuse of AIP content is subject to the terms at: http://scitation.aip.org/termsconditions. Downloaded to IP: 132.239.69.167 On: Wed, 18 Mar 2015 17:53:47

We choose the time interval τ to be longer than the correlation time but still small enough that $\delta\mathcal{I}_k$ is a small change.

Taylor expanding $D_0[t-\tau,\Gamma']$ with respect to the $\delta\mathcal{I}_k$'s yields the distribution,

$$D(t,\Gamma) \simeq D_0(t-\tau,\Gamma) + \sum_{h=1}^{2}\alpha_h D_0(t-\tau,\Gamma)\int_{t-\tau}^{t} dt'\{\mathcal{I}_h,\mathcal{H}\}|_{\Gamma'(\Gamma,t'-t)}. \tag{46}$$

When this distribution is substituted into integrand (42), the first term integrates to zero according to Eq. (44). Since the thermodynamic variables change only by a small amount during the time τ, $D_0(t-\tau,\Gamma)$ may be approximated by $D_0(t,\Gamma)$ in the second term yielding the result

$$\frac{d\langle\mathcal{I}_k\rangle}{dt} = \sum_{h=1}^{2}\alpha_h\int_{t-\tau}^{t} dt'\int d\Gamma D_0(t,\Gamma)\{\mathcal{I}_k,\mathcal{H}\}|_{\Gamma}\{\mathcal{I}_h,\mathcal{H}\}|_{\Gamma'(\Gamma,t'-t)}. \tag{47}$$

The Poisson brackets in Eq. (47) are non-zero only in regions of Γ-space corresponding to close, well-separated, binary collisions. In those regions, the Poisson brackets depend primarily on the coordinates and velocities of the two colliding particles. Thus, the coordinates of all the other particles may be integrated out, reducing Eq. (47) to the form

$$\begin{aligned}\frac{d\langle\mathcal{I}_k\rangle}{dt} = {}& \alpha_k\frac{N_k(N_k-1)}{2}\int_{t-\tau}^{t} dt'\int d\gamma\mathcal{F}(1_k,2_k)\{I(1_k)+I(2_k),H(1_k,2_k)\}|_{\gamma}\cdot\{I(1_k)+I(2_k),H(1_k,2_k)\}|_{\gamma'=\gamma'(\gamma,t'-t)}\\ &+\alpha_k N_k N_{k'}\int_{t-\tau}^{t} dt'\int d\gamma\mathcal{F}(1_k,1_{k'})\{I(1_k),H(1_k,1_{k'})\}|_{\gamma}\{I(1_k),H(1_k,1_{k'})\}|_{\gamma'=\gamma'(\gamma,t'-t)}\\ &+\alpha_{k'}N_k N_{k'}\int_{t-\tau}^{t} dt'\int d\gamma\mathcal{F}(1_k,1_{k'})\{I_{(1_k)},H(1_k,1_{k'})\}|_{\gamma}\{I(1_{k'}),H(1_k,1_{k'})\}|_{\gamma'=\gamma'(\gamma,t'-t)}.\end{aligned} \tag{48}$$

Here $k'=2$ if $k=1$ and $k'=1$ if $k=2$. The two-particle function $\mathcal{F}(i_k,j_q)$ is obtained by integrating $D(\Gamma)$ over coordinates and velocities for all particles except i_k and j_q, and $H(i_k,j_q)$ is the two-particle Hamiltonian governing the collisions between i_k and j_q (see Eq. (12) of Sec. II). The first term in Eq. (48) describes a collision between particles 1 and 2 of species k, and there are $N_k(N_k-1)/2$ such collisions. The next two terms describe a collision between particle 1 of species k and particle 1 of species k', and there are $N_kN_{k'}$ such collisions. If for brevity we refer to particles i_k and j_q as particles 1 and 2, the two-particle phase-space volume element $d\gamma$ is given by

$$\begin{aligned}d\gamma &= dz_1dp_1dz_2dp_2d\psi_1dI_1d\psi_2dI_2dY_1dP_{Y_1}dY_2dP_{Y_2}\\ &= (m_km_q)^3dzdv_zdZdV_zd\psi_1d\psi_2v_{\perp1}dv_{\perp1}v_{\perp2}dv_{\perp2}\\ &\quad\times dX_1dY_1dX_2dY_2,\end{aligned} \tag{49}$$

where use has been made of the definitions $I_j = m_jv_{\perp j}^2/(2\Omega_j)$ and $P_{Y_j} = m_j\Omega_jX_j$, and where (z,v_z) are the relative position and velocity in z and (Z,V_z) are the center of mass position and velocity. These latter two variables do not enter the Poisson brackets.

Next, we argue that the $t'-t$ dependence in the $d\gamma$-integrals of Eq. (48) is even in $t'-t$. From Hamiltonian (14), we see that the Poisson brackets in Eq. (48) involve terms of the form $g_{\mu\nu}\exp[i\mu\psi_1+i\nu\psi_2]$. The dependence on $t'-t$ enters because the second bracket in each product of brackets is evaluated at the primed phase point $\Gamma'=\Gamma'(\Gamma,t'-t)$. When the products of brackets are averaged over the random initial phases of the gyroangles, the resulting time dependence from the gyroangles is of the form $\cos[\mu(\psi_1'-\psi_1)+\nu(\psi_2'-\psi_2)] = \cos[(\mu\Omega_1+\nu\Omega_2)(t'-t)]$, which is even in $(t'-t)$. The remaining time dependence comes from the relative coordinate $z'=z'(z,t'-t)$, which enters $g_{\mu\nu}(\gamma')$. From Eq. (23), one can see that z' is unchanged for $(t'-t)\to-(t'-t)$ and $v_\parallel\to-v_\parallel$, where $v_\parallel$ is the value of the relative velocity v_z before the interaction. This is seen most simply for the simple case where the particles stream without interaction and $z'=z+v_z(t'-t)$. Of course, $f(\gamma)$ is invariant under the interchange $v_z\to-v_z$, so the $d\gamma$-integrals are even in $(t'-t)$.

Thus, the integral $\int_{t-\tau}^{t}dt'$ in Eq. (48), can be replaced by the integral $\frac{1}{2}\int_{t-\tau}^{t+\tau}dt'$. The dt' integral then extends over the full duration of a collision, and Eq. (48) can be rewritten as

$$\begin{aligned}\frac{d\langle\mathcal{I}_k\rangle}{dt} = \frac{1}{2}\Bigg\{&\alpha_k\frac{N_k(N_k-1)}{2}\int d\gamma\mathcal{F}(1_k,2_k)\{I(1_k)+I(2_k),H(1_k,2_k)\}\Delta(I(1_k)+I(2_k))_{(1_k,2_k)}\\ &+\alpha_kN_kN_{k'}\int d\gamma\mathcal{F}(1_k,1_{k'})\{I(1_k),H((1_k,1_{k'}))\}\Delta(I(1_k))_{(1_k,1_{k'})}\\ &+\alpha_{k'}N_kN_{k'}\int d\gamma\mathcal{F}(1_k,1_{k'})\{I(1_k),H((1_k,1_{k'}))\}\Delta(I(1_{k'}))_{(1_k,1_{k'})}\Bigg\},\end{aligned} \tag{50}$$

This article is copyrighted as indicated in the article. Reuse of AIP content is subject to the terms at: http://scitation.aip.org/termsconditions. Downloaded to IP: 132.239.69.167 On: Wed, 18 Mar 2015 17:53:47

where

$$\Delta(I(1_k)+I(2_k))_{(1_k,2_k)} \equiv \int_{t-\tau}^{t+\tau} dt' \{I(1_k) + I(2_k), H(1_k,2_k)\}|_{\gamma'=\gamma'(\gamma,t'-t)} \quad (51)$$

is the change in $(I(1_k) + I(2_k))$ during a collision between particles 1_k and 2_k. The quantities $\Delta(I(1_k))_{(1_k,1_{k'})}$ and $\Delta(I(1_{k'}))_{(1_k,1_{k'})}$ follow the same notation. These changes were evaluated in Sec. II.

Next, we note that one coordinate in the $d\gamma$-integral can be written as a time integral. Figure 6 shows the (z,v_z) phase space with a typical trajectory for a collision. Such a trajectory is described by Eq. (23). The $d\gamma$-integral includes an integral over the $dzdv_z$ plane, and we propose to carry out the integral by arranging area elements in a sequence along each phase in the trajectory using the incompressible nature of the flow, $dz'dv_z' = dzdv_z$. Along the trajectory, the two-particle distribution $\mathcal{F}$ is a constant, so it may be evaluated at some starting area element before the interaction, say at $dzdv_z$. At this starting element we set $dz = |v_z|dt$, where $|v_z|$ is the initial relative velocity defined in Eq. (23). Thus for each element along the trajectory, we have the integration element $dz'dv_z' = |v_z|dtdv_z$. The time integral dt is an integral of the Poisson bracket along the trajectory, that is, over the course of the collision, and yields the change in the actions during the collision. Thus, Eq. (50) reduces to the form

$$\frac{d\langle \mathcal{I}_k\rangle}{dt} = \frac{1}{2}\left\{\alpha_k \frac{N_k(N_k-1)}{2}\int d\tilde{\gamma}\mathcal{F}^{(0)}[\Delta(I(1_k)+I(2_k))_{(1_k,2_k)}]^2 + \alpha_k N_k N_{k'}\int d\tilde{\gamma}\mathcal{F}^{(0)}[\Delta(I(1_k))_{(1_k,1_{k'})}]^2 + \alpha_{k'}N_kN_{k'}\int d\tilde{\gamma}\mathcal{F}^{(0)}[\Delta(I(1_k))_{(1_k,1_{k'})}][\Delta(I(1_{k'}))_{(1_k,1_{k'})}]\right\}, \quad (52)$$

where $\mathcal{F}^{(0)}$ is the distribution evaluated at a phase point before the interaction and

$$d\tilde{\gamma} = \frac{d\gamma}{dt} = (m_k m_q)^3 |v_z| dv_z dZ dV_z d\psi_1 d\psi_2 v_{\perp 1} dv_{\perp 1} v_{\perp 2} dv_{\perp 2} \times dX_1 dY_1 dX_2 dY_2. \quad (53)$$

Here, the subscripts 1 and 2 stand for i_k and j_q as in Eq. (48).

In this same notation, the distribution before the interaction is given by

$$\mathcal{F}^{(0)} = C\exp\left[-\frac{H(1,2)}{T_\parallel} - \alpha_1 I_1 - \alpha_2 I_2\right], \quad (54)$$

where C is a normalization constant and

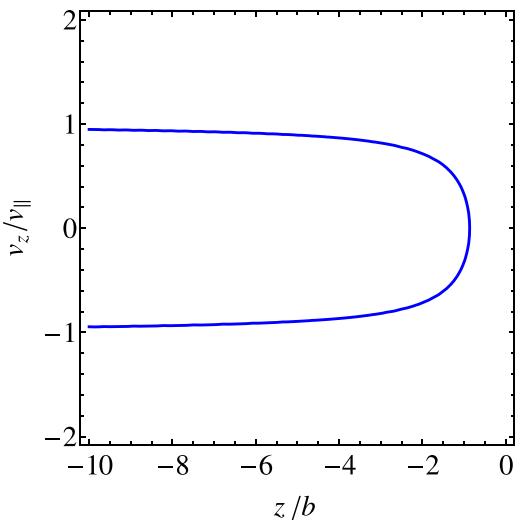

FIG. 6. A typical trajectory for a collision in the (z,v_z) plane. Here, b is the distance of closest approach, and $v_\parallel$ is the velocity at $t = \pm\infty$.

$$H(1,2) = \frac{m_k}{2}(v_{z1}^2 + v_{\perp 1}^2) + \frac{m_q}{2}(v_{z2}^2 + v_{\perp 2}^2) = \frac{\mu_{kq}v_z^2}{2} + \frac{M_{kq}V_z^2}{2} + \frac{m_k v_{\perp 1}^2}{2} + \frac{m_q v_{\perp 2}^2}{2}. \quad (55)$$

Here, $\mu_{kq} = m_k m_q/(m_k + m_q)$ is the reduced mass and $M_{kq} = m_k + m_q$ is the total mass of the two particles. From the normalization $\int d\gamma \mathcal{F}^{(0)} = 1$, we find the distribution

$$\mathcal{F}^{(0)} = \frac{1}{L^6(m_k m_q)^3(2\pi)^2}\frac{\sqrt{m_k m_q}}{2\pi T_\parallel}\frac{m_k m_q}{T_{\perp k}T_{\perp q}} \times \exp\left(-\frac{\mu_{kq}v_z^2}{2T_\parallel} - \frac{M_{kq}V_z^2}{2T_\parallel} - \frac{m_k v_{\perp 1}^2}{2T_{\perp k}} - \frac{m_q v_{\perp 2}^2}{2T_{\perp q}}\right), \quad (56)$$

where L^3 is the volume of the plasma and $T_{\perp k} = T_\parallel/(1 + \alpha_k T_\parallel/\Omega_k)$.

It is convenient to define the relative, parallel thermal velocity of a species i particle and a species j particle as

$$\bar{v}_{ij} = \sqrt{\frac{T_\parallel}{\mu_{ij}}}, \quad (57)$$

and the magnetization of a species- i particle in interaction with a species-j particle as

$$\bar{\kappa}_{ij} = \frac{\bar{b}\Omega_i}{\bar{v}_{ij}}, \quad (58)$$

where the distance of closest approach is $\bar{b} = 2e^2/T_\parallel$.

Note that because of this definition, the $\bar{\kappa}_{ij}$'s are related to $\bar{\kappa}_{11}$ by ratios of masses

$$\bar{\kappa}_{ij} = \bar{\kappa}_{11}\frac{m_1}{m_i}\sqrt{\frac{2m_i/m_1}{(1+m_i/m_j)}}. \quad (59)$$

This article is copyrighted as indicated in the article. Reuse of AIP content is subject to the terms at: http://scitation.aip.org/termsconditions. Downloaded to IP: 132.239.69.167 On: Wed, 18 Mar 2015 17:53:47

Specifically,

$$\bar{\kappa}_{22} = \bar{\kappa}_{11}\left(\frac{m_1}{m_2}\right)^{1/2}, \tag{60}$$

$$\bar{\kappa}_{12} = \bar{\kappa}_{11}\sqrt{\frac{2}{(1+m_1/m_2)}}, \tag{61}$$

$$\text{and } \bar{\kappa}_{21} = \bar{\kappa}_{11}\frac{m_1}{m_2}\sqrt{\frac{2}{(1+m_1/m_2)}}. \tag{62}$$

According to Eqs. (32)–(34), the change in actions depend on the initial gyroangles ϕ_1 and ϕ_2. Along any trajectory of the kind shown in Fig. 6, the gyroangle ϕ_j differs from the ψ_j in the differential for $d\bar{\gamma}$ only by a constant, so we can replace $d\psi_1 d\psi_2$ in the differential with $d\phi_1 d\phi_2$. Also, the change in actions depend on X_1, Y_1, X_2, Y_2 only through $\eta = |\Delta\mathbf{R}_\perp|/b$, where $|\Delta\mathbf{R}_\perp|^2 = (X_1 - X_2)^2 + (Y_1 - Y_2)^2$, so in the differential $d\bar{\gamma}$ we set $dX_1 dY_1 dX_2 dY_2 = 2\pi b^2 \eta d\eta dX_2 dY_2$. The integral over $dZdX_2dY_2$ then trivially gives a factor of L^3. The change in actions does not depend on V_z, so the V_z integral yields $\sqrt{2\pi T_z/M_{kq}}$. When substituting Eq. (56) for $\mathcal{F}^{(0)}(1,2)$, one must be careful to identify the species of particles 1 and 2. For example, in the first term of Eq. (52) both 1 and 2 are of species k, and in the second and third terms, particles 1 and 2 are of species k and k'. Making these substitutions and using the relations $\mathcal{I}_k = N_k T_{\perp k}/\Omega_k$ and $\alpha_k/\Omega_k = (1/T_{\perp k} - 1/T_\parallel)$ yields the result

$$\begin{aligned}\frac{dT_{\perp k}}{dt} = (T_\parallel - T_{\perp k})&\left[n_k \bar{b}^2 \bar{v}_{kk} \cdot \frac{\sqrt{2\pi}}{8}\Lambda_1(\bar{\kappa}_{kk})\right.\\ &\left. + n_{k'}\bar{b}^2\bar{v}_{kk'}\cdot\frac{\sqrt{2\pi}}{4}\frac{\mu_{kk'}}{m_k}\Lambda_1(\bar{\kappa}_{kk'})\right]\\ &+ \frac{(\alpha_k - \alpha_{k'})T_{\perp k}T_{\perp k'}}{\Omega_{k'}}\cdot\frac{\mu_{kk'}^2}{m_k m_{k'}}\\ &\times\frac{n_{k'}\bar{b}^2\bar{v}_{kk'}}{\bar{\kappa}_{kk'}\bar{\kappa}_{k'k}}\frac{\sqrt{2\pi}}{2}\Lambda_2(|\bar{\kappa}_{kk'} - \bar{\kappa}_{k'k}|),\end{aligned} \tag{63}$$

where

$$\Lambda_1(\bar{\kappa}) = \int_0^\infty \frac{d\sigma}{\sigma}\int_0^\infty \eta^3 d\eta f_1^2\left(\frac{\bar{\kappa}}{\sigma^3},\eta\right)e^{-\sigma^2/2} \tag{64}$$

$$\Lambda_2(\bar{\kappa}) = \int_0^\infty d\sigma\sigma^3\int_0^\infty \eta d\eta f_2^2\left(\frac{\bar{\kappa}}{\sigma^3},\eta\right)e^{-\sigma^2/2}. \tag{65}$$

In Appendix A, we obtain the large $\bar{\kappa}$ asymptotic limits

$$\Lambda_1(\bar{\kappa}) = 3.10\bar{\kappa}^{-7/15}e^{-5(3\pi\bar{\kappa})^{2/5}/6}, \tag{66}$$

$$\Lambda_2(\bar{\kappa}) = 3.87\bar{\kappa}^{13/15}e^{-5(3\pi\bar{\kappa})^{2/5}/6}. \tag{67}$$

For the strong magnetization ordering $\bar{\kappa}_{ij} \gg |\bar{\kappa}_{12} - \bar{\kappa}_{21}| \gg 1$, we note that $\Lambda_1(\bar{\kappa}_{ij}) \ll \Lambda_2(|\bar{\kappa}_{12} - \bar{\kappa}_{21}|)$.

Here, the last term on the Right Hand Side of Eq. (63) describes the rapid relaxation where particles of species k collide with particles of species k' and exchange cyclotron actions. As one would expect, this term is proportional to $(\alpha_k - \alpha_{k'})$ and vanishes when $\alpha_k = \alpha_{k'}$. The first term describes the slow relaxation where the total cyclotron action is broken and liberated (or absorbed) cyclotron energy is exchanged with parallel energy. As one would expect, this term is proportional to $T_\parallel - T_{\perp k}$, and vanishes when $T_\parallel = T_{\perp k}$. Note here that $(T_\parallel - T_{\perp k})$ is proportional to α_k, so one may equally say that the term vanishes when $\alpha_k = 0$. Also, note that when the two species are the same (i.e., when $k = k'$) and when $\alpha_k = \alpha_{k'}$, the rate equation reduces to that obtained in the work of O'Neil and Hjorth.[4] Finally, we will argue in Sec. IV that Eq. (63) is an easy place to generalize the treatment to more than two species. One simply sums k' over all species except $k' = k$.

Next, we introduce scaled variables. The thermodynamic variables $T_\parallel$, α_1 and α_2 are the three unknowns, which we scale as $\hat{T}_\parallel = T_\parallel/T_{\parallel 0}$ and $\hat{\alpha}_k = \alpha_k T_{\parallel 0}/\Omega_1$, where $T_{\parallel 0} = T_\parallel(0)$ is the initial value of $T_\parallel$. An equivalent set of thermodynamic variables is the three temperatures $T_\parallel$, $T_{\perp 1}$ and $T_{\perp 2}$; we scale the perpendicular temperatures as $\hat{T}_{\perp k} = T_{\perp k}/T_{\parallel 0}$. $\hat{\alpha}_k$ and $\hat{T}_{\perp k}$ are related by $\hat{\alpha}_k = (m_1/m_k)(1/\hat{T}_{\perp k} - 1/\hat{T}_\parallel)$. The actions are scaled as $\langle\hat{\mathcal{I}}_k\rangle = \langle\mathcal{I}_k\rangle(\Omega_1/T_{\parallel 0})$. We introduce a scaled time $\hat{t} = tn\bar{b}_0^2\bar{v}_{11,0}$, where again subscripts zero refer to initial values and $n\bar{b}^2\bar{v}_{11} = n\bar{b}_0^2\bar{v}_{11,0}(T_{\parallel 0}/T_\parallel)^{3/2}$. The magnetization parameter $\bar{\kappa}_{ij}$ is already dimensionless, but does have a temperature dependence $\bar{\kappa}_{ij} = \bar{\kappa}_{ij,0}(T_{\parallel 0}/T_\parallel)^{3/2}$. Following the same notation, we write density ratios as $\hat{n}_k = n_k/n$ The scaling removes dependence on the total density n, and dependence on B enters only in the combination with $T_{\parallel 0}$ through the magnetization parameter $\bar{\kappa}_{11,0}$. As we will see, the solution depends only on the initial values of the scaled thermodynamic variables, the initial magnetization strength $\bar{\kappa}_{11,0} = \Omega_1\bar{b}_0/\bar{v}_{11,0}$, the mass ratio m_1/m_2, and the density ratios $\hat{n}_k = n_k/n$.

In terms of these scaled variables, Eq. (63) takes the form

$$\frac{d\hat{T}_{\perp k}}{d\hat{t}} = \left[\hat{\alpha}_k\frac{\hat{G}_k}{\hat{n}_k} + (\hat{\alpha}_k - \hat{\alpha}_{k'})\frac{\hat{K}_k}{\hat{n}_k}\right]\frac{m_1}{m_k}, \tag{68}$$

where

$$\begin{aligned}\hat{G}_k = &\frac{\hat{T}_{\perp k}}{\hat{T}_\parallel^{1/2}}\cdot\left(\frac{m_k}{m_1}\right)^{3/2}\frac{\sqrt{2\pi}}{8}\\ &\times\left[\hat{n}_k^2\Lambda_1(\bar{\kappa}_{kk}) + \hat{n}_k\hat{n}_{k'}\sqrt{\frac{2}{1+m_k/m_{k'}}}\Lambda_1(\bar{\kappa}_{kk'})\right]\end{aligned} \tag{69}$$

regulates equipartition of $\hat{T}_{\perp k}$ with $\hat{T}_\parallel$ on the slower timescale, and

$$\begin{aligned}\hat{K}_k = &\frac{\hat{T}_{\perp k}\hat{T}_{k'}}{\hat{T}_\parallel^{3/2}}\cdot\hat{n}_k\hat{n}_{k'}\frac{\sqrt{2\pi}}{8}\cdot\sqrt{\left(\frac{m_k}{m_1}\frac{m_{k'}}{m_1}\right)^3\frac{2m_1}{m_k+m_{k'}}}\\ &\times\frac{\Lambda_2(|\bar{\kappa}_{kk'} - \bar{\kappa}_{k'k}|)}{\bar{\kappa}_{11}^2}\end{aligned} \tag{70}$$

regulates equipartition of α_k with $\alpha_{k'}$ on the faster timescale. The statement of conservation of energy in Eq. (41) can be rewritten as the relation,

This article is copyrighted as indicated in the article. Reuse of AIP content is subject to the terms at: http://scitation.aip.org/termsconditions. Downloaded to IP: 132.239.69.167 On: Wed, 18 Mar 2015 17:53:47

$$\hat{T}_{\parallel}(t) = 1 + 2\{\hat{n}_1[\hat{T}_{\perp 1}(0) - \hat{T}_{\perp 1}(t)] + \hat{n}_2[\hat{T}_{\perp 2}(0) - \hat{T}_{\perp 2}(t)]\}. \tag{71}$$

This equation plus Eq. (68) for $k = 1$ and 2 and the relation $\hat{\alpha}_k = (m_1/m_k)(1/\hat{T}_{\perp k} - 1/\hat{T}_{\parallel})$ determine the evolution of the three unknowns $T_{\parallel}$, $T_{\perp 1}$ and $T_{\perp 2}$ (or equivalently $T_{\parallel}$, α_1 and α_2).

To obtain equations for $\hat{\alpha}_1(t)$ and $\hat{\alpha}_2(t)$ alone, we combine Eq. (68) with the relations

$$\frac{d\hat{\alpha}_k}{d\hat{t}} = \frac{m_1}{m_k}\left(\frac{1}{\hat{T}_{\parallel}^2}\frac{d\hat{T}_{\parallel}}{d\hat{t}} - \frac{1}{\hat{T}_{\perp k}^2}\frac{d\hat{T}_{\perp k}}{d\hat{t}}\right), \tag{72}$$

$$0 = \frac{1}{2}\frac{d\hat{T}_{\parallel}}{d\hat{t}} + \hat{n}_1\frac{d\hat{T}_{\perp 1}}{d\hat{t}} + \hat{n}_2\frac{d\hat{T}_{\perp 2}}{d\hat{t}}. \tag{73}$$

The result is

$$\frac{d\hat{\alpha}_1}{d\hat{t}} = -\hat{\nu}_{11}\hat{\alpha}_1 - \hat{\nu}_{12}\hat{\alpha}_2 - \hat{\Gamma}_1(\hat{\alpha}_1 - \hat{\alpha}_2), \tag{74}$$

$$\frac{d\hat{\alpha}_2}{d\hat{t}} = -\hat{\nu}_{21}\hat{\alpha}_1 - \hat{\nu}_{22}\hat{\alpha}_2 - \hat{\Gamma}_2(\hat{\alpha}_2 - \hat{\alpha}_1), \tag{75}$$

where the $\hat{\nu}_{ij}$'s and the $\hat{\Gamma}_k$'s are given by

$$\hat{\nu}_{ij} = \left(\frac{\delta_{ij}m_1^2}{\hat{T}_{\perp i}^2\hat{n}_i m_i^2} + \frac{2m_1^2}{\hat{T}_{\parallel}^2 m_i m_j}\right)\hat{G}_j, \tag{76}$$

$$\hat{\Gamma}_k = \left[\frac{m_1^2}{\hat{T}_{\perp k}^2\hat{n}_k m_k^2} + \frac{2(1 - m_k/m_{k'})}{\hat{T}_{\parallel}^2 m_k^2/m_1^2}\right]\hat{K}_k, \tag{77}$$

and $\hat{T}_{\perp k} = \hat{T}_{\parallel}/(1 + \hat{\alpha}_k\hat{T}_{\parallel}m_k/m_1)$. In these coefficients, $\hat{T}_{\parallel}(t)$ and $\hat{T}_{\perp k}(t)$ are determined by Eq. (71) and the relation $\hat{T}_{\perp k} = \hat{T}_{\parallel}/(1 + \hat{\alpha}_k\hat{T}_{\parallel}m_k/m_1)$.

Analytic progress in solving Eqs. (74) and (75) is possible in two separate limits. We first discuss the solutions in these limits and then solve the equations numerically for various values of the parameters, verifying the limiting behaviors expected from the analytic solutions.

For sufficiently strong magnetization, the $\hat{K}_k$ and $\hat{G}_j$ integrals satisfy the inequality $\hat{K}_1, \hat{K}_2 \gg \hat{G}_1, \hat{G}_2$, and the collisional relaxation takes place on two timescales. By subtracting Eq. (75) from Eq. (74) and neglecting $\hat{G}_1$ and $\hat{G}_2$ compared to $\hat{K}_1, \hat{K}_2$, we obtain the equation

$$\frac{d}{d\hat{t}}(\hat{\alpha}_1 - \hat{\alpha}_2) = -\hat{\nu}_a(\hat{\alpha}_1 - \hat{\alpha}_2), \tag{78}$$

where

$$\hat{\nu}_a = \hat{\Gamma}_1 + \hat{\Gamma}_2 = \hat{K}_1 \cdot \left[\frac{1}{\hat{T}_{\perp 1}^2\hat{n}_1} + \frac{1}{\hat{T}_{\perp 2}^2\hat{n}_2}\frac{m_1^2}{m_2^2} + \frac{2(1 - m_1/m_2)^2}{\hat{T}_{\parallel}^2}\right] \tag{79}$$

is the rate at which $\hat{\alpha}_1$ and $\hat{\alpha}_2$ relax to a common value $\hat{\alpha}$.

At a slower rate, $\hat{\alpha}$ relaxes to zero. To obtain this rate, we multiply Eq. (74) by $\hat{\Gamma}_2$ and Eq. (75) by $\hat{\Gamma}_1$ and add to obtain the result

$$\hat{\Gamma}_2\frac{d\hat{\alpha}_1}{d\hat{t}} + \hat{\Gamma}_1\frac{d\hat{\alpha}_2}{d\hat{t}} = -\hat{\Gamma}_2(\hat{\nu}_{11}\hat{\alpha}_1 + \hat{\nu}_{12}\hat{\alpha}_2) - \hat{\Gamma}_1(\hat{\nu}_{21}\hat{\alpha}_1 + \hat{\nu}_{22}\hat{\alpha}_2). \tag{80}$$

The large quantity $\hat{K}_1$ enters the $\hat{\Gamma}_j$ on both sides of this equation and cancels, leaving a slow rate of order $\hat{G}_j$. Setting $\hat{\alpha}_1 = \hat{\alpha}_2 = \hat{\alpha}$, then yields the equation

$$\frac{d\hat{\alpha}}{d\hat{t}} = -\hat{\nu}_b\hat{\alpha}, \tag{81}$$

where

$$\hat{\nu}_b = \frac{\hat{\Gamma}_2(\hat{\nu}_{11} + \hat{\nu}_{12})}{\hat{\Gamma}_1 + \hat{\Gamma}_2} + \frac{\hat{\Gamma}_1(\hat{\nu}_{21} + \hat{\nu}_{22})}{\hat{\Gamma}_1 + \hat{\Gamma}_2} = \left\{\sum_{k=1}^{2}\left[\frac{m_1^2/m_{k'}^2}{\hat{T}_{\perp k'}^2\hat{n}_{k'}} + \frac{2m_1/m_{k'}(m_1/m_{k'} - 1)}{\hat{T}_{\parallel}^2}\right] \cdot \left[\frac{2m_1/m_k(1 + m_1/m_k)}{\hat{T}_{\parallel}^2} + \frac{m_1^2/m_k^2}{\hat{T}_{\perp k}^2\hat{n}_k}\right]\hat{G}_k\right\} \cdot \left[\frac{1}{\hat{T}_{\perp 1}^2\hat{n}_1} + \frac{m_1^2/m_2^2}{\hat{T}_{\perp 2}^2\hat{n}_2} + \frac{2(1 - m_1/m_2)^2}{\hat{T}_{\parallel}^2}\right]^{-1} \tag{82}$$

is the rate at which $\hat{\alpha}$ decays to zero, and hence from the relation $\hat{\alpha}_k = (m_1/m_k)(1/\hat{T}_{\perp k} - 1/\hat{T}_{\parallel})$, the rate at which $\hat{T}_{\perp 1}$ and $\hat{T}_{\perp 2}$ approaches $\hat{T}_{\parallel}$.

Of course, this approximate solution is only accurate to order $|\hat{G}_j/\hat{K}_k| \ll 1$. For example, $\hat{\alpha}_1(t) - \hat{\alpha}_2(t)$ does not decay to exactly zero during the first phase of the evolution but rather to the small value $(\hat{\alpha}_1 - \hat{\alpha}_2) \simeq [(\hat{\nu}_{22} + \hat{\nu}_{21} - \hat{\nu}_{11} - \hat{\nu}_{12})/(\hat{\Gamma}_1 + \hat{\Gamma}_2)]\hat{\alpha} \sim \mathcal{O}(\hat{G}_j/\hat{K}_k)\hat{\alpha} \ll \hat{\alpha}$. One can understand this by setting $d\hat{\alpha}_1/d\hat{t}, d\hat{\alpha}_2/d\hat{t} \approx 0$ in Eqs. (74) and (75) and solving for $\hat{\alpha}_1 - \hat{\alpha}_2$.

Another analytic solution is possible when $\hat{\alpha}_1$ and $\hat{\alpha}_2$ are small, and Eqs. (74) and (75) may be treated as linear coupled equations with constant coefficients $\hat{\nu}_{ij}$ and $\hat{\Gamma}_j$. In these coefficients, one must set $\hat{T}_{\parallel} = \hat{T}_{\perp 1} = \hat{T}_{\perp 2} = \hat{T}$. A normal mode analysis[9] then yields the solution

This article is copyrighted as indicated in the article. Reuse of AIP content is subject to the terms at: http://scitation.aip.org/termsconditions. Downloaded to IP: 132.239.69.167 On: Wed, 18 Mar 2015 17:53:47

$$\begin{pmatrix}\hat{\alpha}_1(t)\\ \hat{\alpha}_2(t)\end{pmatrix} = C_+\begin{pmatrix}\hat{\alpha}_{1+}\\ \hat{\alpha}_{2+}\end{pmatrix}e^{\hat{S}_+\hat{t}} + C_-\begin{pmatrix}\hat{\alpha}_{1-}\\ \hat{\alpha}_{2-}\end{pmatrix}e^{\hat{S}_-\hat{t}}, \tag{83}$$

where C_+ and C_- are constants determined by the initial values $\hat{\alpha}_1(0)$ and $\hat{\alpha}_2(0)$, the damping decrements $\hat{S}_+$ and $\hat{S}_-$ are given by

$$\hat{S}_\pm = \frac{1}{2}\Big\{-(\hat{\nu}_{22}+\hat{\nu}_{11}+\hat{\Gamma}_1+\hat{\Gamma}_2)\pm[(\hat{\nu}_{22}+\hat{\nu}_{11}+\hat{\Gamma}_1+\hat{\Gamma}_2)^2 - 4[(\hat{\nu}_{11}\hat{\nu}_{22}-\hat{\nu}_{12}\hat{\nu}_{21}+(\hat{\nu}_{11}+\hat{\nu}_{12})\hat{\Gamma}_2 +(\hat{\nu}_{22}+\hat{\nu}_{21})\hat{\Gamma}_1)]]^{1/2}\Big\}, \tag{84}$$

and the eigenvectors by

$$\begin{pmatrix}\hat{\alpha}_{1+}\\ \hat{\alpha}_{2+}\end{pmatrix} = \begin{pmatrix}\hat{\Gamma}_1-\hat{\nu}_{12}\\ \hat{S}_+ + \hat{\nu}_{11}+\hat{\Gamma}_1\end{pmatrix},\quad \begin{pmatrix}\hat{\alpha}_{1-}\\ \hat{\alpha}_{2-}\end{pmatrix} = \begin{pmatrix}\hat{\Gamma}_1-\hat{\nu}_{12}\\ \hat{S}_- + \hat{\nu}_{11}+\hat{\Gamma}_1\end{pmatrix}. \tag{85}$$

In the strongly magnetized limit where $\hat{\Gamma}_j \gg \hat{\nu}_{ij}$, we recover the previous solution. The damping decrements are approximately

$$\hat{S}_- \simeq -(\hat{\Gamma}_1+\hat{\Gamma}_2),\quad \hat{S}_+ \simeq -\frac{(\hat{\nu}_{11}+\hat{\nu}_{12})\hat{\Gamma}_2+(\hat{\nu}_{22}+\hat{\nu}_{21})\hat{\Gamma}_1}{\hat{\Gamma}_1+\hat{\Gamma}_2}, \tag{86}$$

in agreement with Eqs. (79) and (82). In this limit, the $|+\rangle$ eigenvector is proportional to

$$\begin{pmatrix}\hat{\alpha}_{1+}\\ \hat{\alpha}_{2+}\end{pmatrix} = \begin{pmatrix}1\\ 1+\dfrac{(\hat{\nu}_{11}+\hat{\nu}_{12}-\hat{\nu}_{21}-\hat{\nu}_{22})}{\hat{\Gamma}_1+\hat{\Gamma}_2}\end{pmatrix}, \tag{87}$$

and $[\hat{\alpha}_1(t)-\hat{\alpha}_2(t)]$ evolves to near zero on the timescale $S_-^{-1} \simeq 1/(\Gamma_1+\Gamma_2)$. As mentioned earlier, the correction is of order $(\hat{\nu}_{11}+\hat{\nu}_{12}-\hat{\nu}_{21}-\hat{\nu}_{22})/(\hat{\Gamma}_1+\hat{\Gamma}_2) \sim \mathcal{O}(\hat{G}_j/\hat{K}_k) \ll 1$.

When the $\hat{\Gamma}_k$'s are comparable to the $\hat{\nu}_{ij}$, the separation in timescales between $\hat{S}_+$ and $\hat{S}_-$ no longer exists. This is the case when magnetization is low or the ion mass difference between the two species is large. However, we note again that our rates only apply to the strong magnetization regime $|\bar{\kappa}_{12}-\bar{\kappa}_{21}| \gg 1$. If magnetization is low and $|\bar{\kappa}_{12}-\bar{\kappa}_{21}| \lesssim 1$, the timescale in which particles of different species exchange cyclotron action is comparable to the timescale of a few collisions. Over this timescale, the distribution would not be cast into the modified Maxwellian in Eq. (38) as assumed.

We convert the rate equations back to unscaled version for easier reference, using the definitions of the scaled physical quantities. The unscaled version of Eqs. (74) and (75) is

$$\frac{d\alpha_k}{dt} = -\nu_{kk}\alpha_k - \nu_{kk'}\alpha_{k'} - \Gamma_k(\alpha_k-\alpha_{k'}), \tag{88}$$

where

$$\nu_{kl} = \left(\frac{2\Omega_k\Omega_l}{nT_\parallel^2}+\frac{\Omega_k^2\delta_{kl}}{n_kT_{\perp k}^2}\right)G_k, \tag{89}$$

$$\Gamma_k = \left[\frac{\Omega_k^2}{n_kT_{\perp k}^2}+\frac{2\Omega_k(\Omega_k-\Omega_{k'})}{nT_\parallel^2}\right]K_k, \tag{90}$$

and

$$G_k = \frac{T_\parallel T_{\perp k}}{\Omega_k^2}\left[n_k^2\bar{b}\bar{v}_{kk}\frac{\sqrt{2\pi}}{8}\Lambda_1(\bar{\kappa}_{kk}) + n_kn_{k'}\bar{b}\bar{v}_{kk'}\frac{\sqrt{2\pi}}{4}\frac{\mu_{kk'}}{m_k}\Lambda_1(\bar{\kappa}_{kk'})\right], \tag{91}$$

$$K_k = \frac{T_{\perp k}T_{\perp k'}}{\Omega_k\Omega_{k'}}\frac{\mu_{kk'}^2}{m_km_{k'}}\frac{n_kn_{k'}\bar{b}^2\bar{v}_{kk'}}{\bar{\kappa}_{kk'}\bar{\kappa}_{k'k}}\frac{\sqrt{2\pi}}{2}\Lambda_2(|\bar{\kappa}_{kk'}-\bar{\kappa}_{k'k}|). \tag{92}$$

Then in the first stage of equilibration,

$$\frac{d}{dt}(\alpha_1-\alpha_2) = -\nu_a(\alpha_1-\alpha_2), \tag{93}$$

where

$$\nu_a = \left[\frac{\Omega_1^2}{n_1T_{\perp 1}^2}+\frac{\Omega_2^2}{n_2T_{\perp 2}^2}+\frac{2(\Omega_1-\Omega_2)^2}{nT_\parallel^2}\right]K_1. \tag{94}$$

And then in the next stage of equilibration, where $\alpha_1 = \alpha = \alpha_2$

$$\frac{d\alpha}{dt} = -\nu_b\alpha, \tag{95}$$

where

$$\nu_b = \frac{\Gamma_2(\nu_{11}+\nu_{12})+\Gamma_1(\nu_{21}+\nu_{22})}{\Gamma_1+\Gamma_2} = \left[\sum_{k=1}^{2}\left(\frac{2\Omega_{k'}(\Omega_{k'}-\Omega_k)}{nT_\parallel^2}+\frac{\Omega_{k'}^2}{n_{k'}T_{\perp k'}^2}\right)\times\left(\frac{2\Omega_k(\Omega_k+\Omega_{k'})}{nT_\parallel^2}+\frac{\Omega_k^2}{n_kT_{\perp k}^2}\right)G_k\right]\times\left[\frac{\Omega_1^2}{n_1T_{\perp 1}^2}+\frac{\Omega_2^2}{n_2T_{\perp 2}^2}+\frac{2(\Omega_1-\Omega_2)^2}{nT_\parallel}\right]^{-1}. \tag{96}$$

Next, we consider three numerical integrations of (74) and (75). For both the first and the second integrations, we choose $\hat{n}_1 = \hat{n}_2 = 1/2$ for convenience, and $m_2/m_1 = 25/24$, as that is the mass ratio of two common constituent ions in a pure ion plasma, namely Mg_{25}^+ and Mg_{24}^+.[6,7] For all the cases, the lighter ion has a mass of $m_1 = 24m_p$, where m_p is the proton mass. We choose the total density to be $n = 10^5\ \mathrm{cm}^{-3}$. The parallel temperature $T_\parallel$ is assumed to be in the range where the plasma is weakly correlated, i.e., $\Gamma_{\mathrm{corr}} < 1$, where $\Gamma_{\mathrm{corr}} = (4\pi n/3)^{1/3}e^2/T_\parallel$ is the coupling parameter.[14] This requires $T_\parallel > 1.1\times10^{-5}$ eV. We also choose the magnetic field to be $B = 60$ kG, a value that was realized in past experiments.[1,2]

This article is copyrighted as indicated in the article. Reuse of AIP content is subject to the terms at: http://scitation.aip.org/termsconditions. Downloaded to IP: 132.239.69.167 On: Wed, 18 Mar 2015 17:53:47

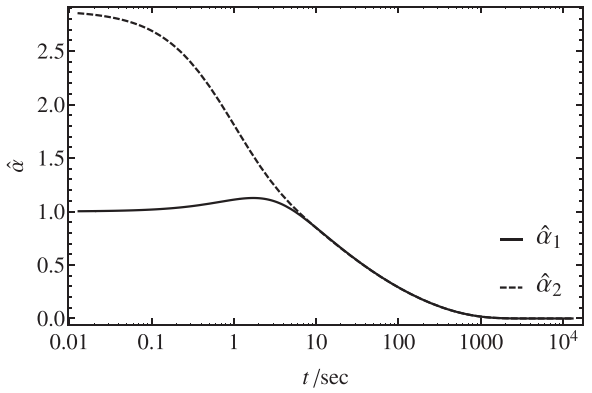

FIG. 7. The time evolution of $\hat{\alpha}_1$ and $\hat{\alpha}_2$ for the case of $\bar{\kappa}_{11,0} = 80.0$, $m_2/m_1 = 25/24$ and $\hat{n}_1 = \hat{n}_2 = .5$. Here, $n\bar{b}_0^2\bar{\nu}_{11,0} = 7.7 \times 10^3\ \mathrm{s}^{-1}$ and $T_{\|0} = 4.5 \times 10^{-5}$ eV.

The first integration is for a case of strong magnetization $\bar{\kappa}_{11,0} = 80.0$ and correspondingly $\bar{\kappa}_{12,0} - \bar{\kappa}_{21,0} = 3.2$. The initial parallel temperature $T_{\|0}$ under this value of $\bar{\kappa}_{11,0}$ is 4.5×10^{-5} eV. With this temperature, the system has a weak correlation of $\Gamma_{\mathrm{corr}} = 0.24$. For such a density and temperature, the collision rate is $n\bar{b}_0^2\bar{\nu}_{11,0} = 7.7 \times 10^3\ \mathrm{s}^{-1}$. Also, the initial scaled perpendicular temperatures are taken to be $\hat{T}_{\perp 1,0} = 0.5$ and $\hat{T}_{\perp 2,0} = 0.25$. The evolution of $\hat{\alpha}_1$ and $\hat{\alpha}_2$ is shown in Fig. 7 and of $\hat{T}_{\perp 1}, \hat{T}_{\perp 1}$ and $\hat{T}_{\|}$ in Fig. 8. In this case, the separation of timescales is clearly apparent. $\hat{\alpha}_1$ and $\hat{\alpha}_2$ evolve to a common value in a time of 10 s and then evolve to zero in the longer time of 1000 s, or 17 min. Note in both figures that the abscissa is a logarithmic scale. As $T_{\|}$ decreases during the final relaxation, the magnetization $\bar{\kappa}_{11} \propto T_{\|}^{-3/2}$ rises and the equipartition rate, which has the $\exp[-5(3\pi\bar{\kappa}_{11}^{2/5})/6]$ dependence, is exponentially suppressed. This accounts for the fact that the final equipartition takes place over a long three decades of time. In Fig. 8, the temperatures $\hat{T}_{\perp 1}$ and $\hat{T}_{\perp 2}$ have slightly different values even after $\hat{\alpha}_1$ and $\hat{\alpha}_2$ have reached common value because of the mass dependence in the relation $\hat{T}_{\perp k} = \hat{T}_{\|}(1 + \hat{\alpha}_k\hat{T}_{\|}m_k/m_1)$. Note that the correction in Eq. (87) is not visible on the scale of the figures.

The second case, as shown in Figs. 9 and 10, is for a case where the initial parallel temperature is lower than the perpendicular temperatures, but the magnetization and ion masses stay the same as in the first case. The first

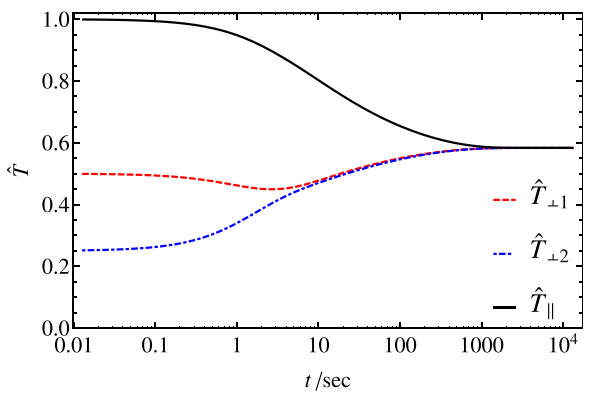

FIG. 8. The time evolution of $\hat{T}_{\perp 1}, \hat{T}_{\perp 2}$ and $\hat{T}_{\|}$ for the case of $\bar{\kappa}_{11,0} = 80.0$, $m_2/m_1 = 25/24$ and $\hat{n}_1 = \hat{n}_2 = .5$. Here, $n\bar{b}_0^2\bar{\nu}_{11,0} = 7.7 \times 10^3\ \mathrm{s}^{-1}$ and $T_{\|0} = 4.5 \times 10^{-5}$ eV.

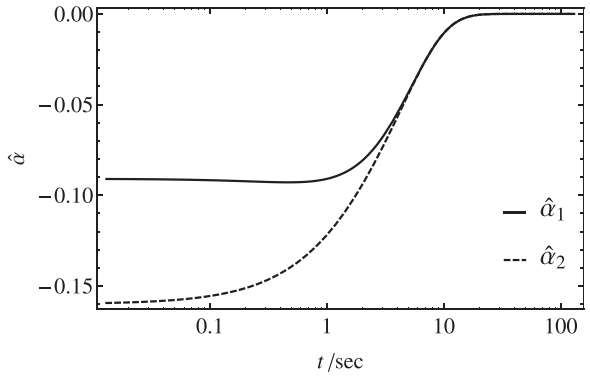

FIG. 9. The time evolution of $\hat{\alpha}_1$ and $\hat{\alpha}_2$ for the case of $\bar{\kappa}_{11,0} = 80.0$, $m_2/m_1 = 25/24$ and $\hat{n}_1 = \hat{n}_2 = .5$. Here $n\bar{b}_0^2\bar{\nu}_{11,0} = 7.7 \times 10^3\ \mathrm{s}^{-1}$ and $T_{\|0} = 4.5 \times 10^{-5}$ eV.

equipartition, when $\hat{\alpha}_1$ and $\hat{\alpha}_2$ are approaching to the same value, has similar duration as in the previous case, but the final equipartition occurs over an exponentially much shorter duration of 20 s than in that previous case, as the increase in parallel temperature speeds up equipartition exponentially.

The third integration is for a case of strong magnetization, but large ion mass difference between the two species. $\bar{\kappa}_{11,0} = 80.0$ and $\bar{\kappa}_{12,0} - \bar{\kappa}_{21,0} = 24.7$, with a choice of $m_2/m_1 = 1.4$. The values of n and $T_{\|,0}$ are the same as in the previous cases. In this case, the rate $\hat{\nu}_a \sim \mathcal{O}(\exp[-5(3\pi|\bar{\kappa}_{12} - \bar{\kappa}_{21}|^{2/5})/6]/\bar{\kappa}_{11}^2)$ of the first equipartition is comparable to the rate $\hat{\nu}_b \sim \mathcal{O}(\exp[-5(3\pi\bar{\kappa}_{11}^{2/5})/6])$ of the second stage. The thermodynamic variables $\hat{\alpha}_1$ and $\hat{\alpha}_2$ decay to zero without equilibrating first to a common value, and the temperatures $\hat{T}_{\|}$, $\hat{T}_{\perp 1}$ and $\hat{T}_{\perp 2}$ converge to the same value, as in Figs. 11 and 12.

IV. DISCUSSION

The analysis of Sec. III assumes that the ion plasma is immersed in a uniform neutralizing background charge. For the case of a single species ion plasma, a laboratory realization of this simple theoretical model is a pure ion plasma in a Malmberg-Penning trap.[17] Rotation of the plasma in the uniform axial magnetic field of the trap induces a radial electric field and a radial centrifugal force that can be thought of as arising from an imaginary cylinder of uniform neutralizing

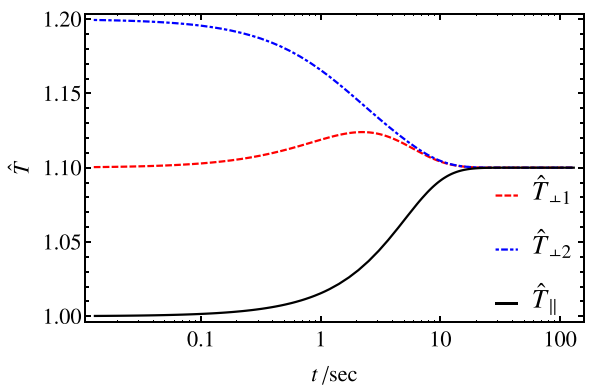

FIG. 10. The time evolution of $\hat{T}_{\perp 1}, \hat{T}_{\perp 2}$ and $\hat{T}_{\|}$ for the case of $\bar{\kappa}_{11,0} = 80.0$, $m_2/m_1 = 25/24$, and $\hat{n}_1 = \hat{n}_2 = .5$. Here, $n\bar{b}_0^2\bar{\nu}_{11,0} = 7.7 \times 10^3\ \mathrm{s}^{-1}$ and $T_{\|0} = 4.5 \times 10^{-5}$ eV.

This article is copyrighted as indicated in the article. Reuse of AIP content is subject to the terms at: http://scitation.aip.org/termsconditions. Downloaded to IP: 132.239.69.167 On: Wed, 18 Mar 2015 17:53:47

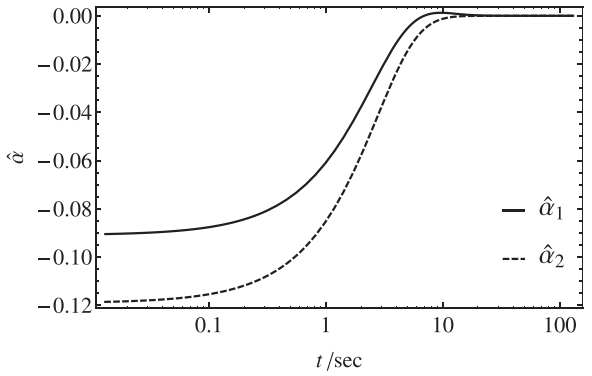

FIG. 11. The time evolution of $\hat{\alpha}_1$ and $\hat{\alpha}_2$ for the case of $\bar{\kappa}_{11,0} = 80.0$ and $|\bar{\kappa}_{21,0} - \bar{\kappa}_{12,0}| = 24.7$. Here, $m_2/m_1 = 1.4$, $\hat{n}_1 = \hat{n}_2 = .5$, $n\bar{b}_0^2\bar{\nu}_{11,0} = 7.7 \times 10^3\ \mathrm{s}^{-1}$ and $T_{\|0} = 4.5 \times 10^{-5}$ eV.

background charge.[14,18] The Gibb's distribution for the magnetically confined single-species plasma differs only by rigid rotation from that for a plasma confined by a cylinder of neutralizing charge.[14,18]

However, there is a caveat to this equivalence for the case of a pure ion plasma with different mass species. The rotation can give rise to centrifugal separation of the species.[6,19,20] A parameter that determines the degree of separation is the quantity $\omega^2|m_2 - m_1|r_p^2/T_\|$, where ω is the plasma rotation frequency and r_p is the radius of the cylindrical plasma column. We assume that this quantity is small compared to unity so that centrifugal separation is negligible and the equivalence is preserved. Note that ω varies inversely with magnetic field strength,[14] so small $\omega^2|m_2 - m_1|r_p^2/T_\|$ can be consistent with strong magnetization.

For a plasma in a Malmberg-Penning trap, the Hamiltonian $\mathcal{H}$ and the actions $\mathcal{I}_k$ are to be interpreted as the Hamiltonian and actions in the rotating frame of the plasma. To be precise, the actions are defined in the local drift frame,[21] but for the plasmas of interest, the difference between the local drift velocity and the local plasma velocity (i.e., $r\omega$) is negligibly small, that is, small compared to the thermal velocity.

Another caveat concerns the statement of conservation of kinetic energy in Eq. (63). In some experiments heating processes have rates that are comparable to the rate at which the α_k's relax. If the heating process is understood and the rate can be quantified in a formula, the heating rate should replace the zero on the Left Hand Side of Eq. (73). Alternatively, one can proceed empirically and measure $T_\|(t)$, say using Laser Induced Fluorescence,[17] and then use Eq. (63) to determine the evolution of $T_{\perp 1}(t)$ and $T_{\perp 2}(t)$, or equivalently of $\alpha_1(t)$ and $\alpha_2(t)$. Of course, the relaxation of the α's can occur on two timescales, and it may be that the heating is negligible for the relatively rapid relaxation of $\alpha_1(t)$ and $\alpha_2(t)$ to a common value, but not negligible on the longer timescale where that common value relaxes to zero.

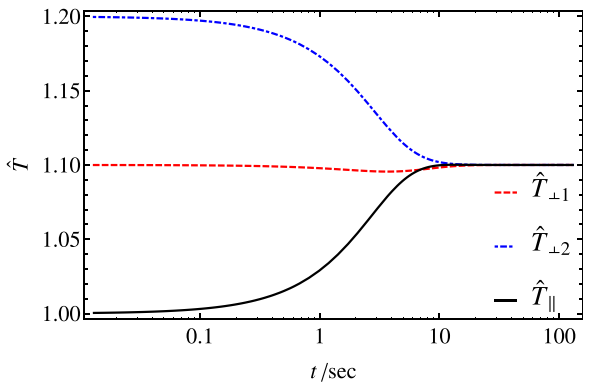

FIG. 12. The time evolution of $\hat{T}_{\perp 1}, \hat{T}_{\perp 2}$ and $\hat{T}_\|$ for the case of $\bar{\kappa}_{11,0} = 80.0$ and $|\bar{\kappa}_{21,0} - \bar{\kappa}_{12,0}| = 24.7$. Here $m_2/m_1 = 1.4$, $\hat{n}_1 = \hat{n}_2 = .5$, $n\bar{b}_0^2\bar{\nu}_{11,0} = 7.7 \times 10^3\ \mathrm{s}^{-1}$, and $T_{\|0} = 4.5 \times 10^{-5}$ eV.

Finally, there is the question of how the theory should be generalized for the case of three or more isotopic ions. In the discussion following Eq. (63), we noted that this can accomplished by summing the Right Hand Side over k' for $k' \neq k$. In terms of scaled variables, one can sum over k' for subscript $k' \neq k$ on the Right Hand Side of Eq. (68). Note that subscript k' is also implicitly hidden in the expressions (69) and (70) for G_k and K_k. Equation (68) then provides k equations for the $T_{\perp k}$. Also, Eq. (73) for conservation of energy must be modified by summing over terms for each $T_{\perp k}$. This generalization is valid because we keep the assumption of the dominance of uncorrelated binary collisions, among particles of all the k species.

ACKNOWLEDGMENTS

This work was supported by National Science Foundation Grant. No. PHY0903877, U.S. Department of Energy Grant No. DE-SC0002451 and No. DE-SC0008693.

APPENDIX: EVALUATION OF INTEGRALS Λ_1 AND Λ_2

In this Appendix, we evaluate the integrals

$$\Lambda_1(\bar{\kappa}) = \int_0^\infty \frac{d\sigma}{\sigma} \int_0^\infty \eta^3 d\eta f_1^2\left(\frac{\bar{\kappa}}{\sigma^3}, \eta\right) e^{-\sigma^2/2}, \tag{A1}$$

$$\Lambda_2(\bar{\kappa}) = \int_0^\infty d\sigma\sigma^3 \int_0^\infty \eta d\eta f_2^2\left(\frac{\bar{\kappa}}{\sigma^3}, \eta\right) e^{-\sigma^2/2}, \tag{A2}$$

where

$$f_1(\kappa, \eta) = \int_{-\infty}^\infty \frac{\cos(\kappa\xi)d\xi}{[\eta^2 + \zeta^2(\xi)]^{3/2}}, \tag{A3}$$

$$f_2(\kappa, \eta) = \int_{-\infty}^\infty \frac{\cos(\kappa\xi)d\xi}{[\eta^2 + \zeta^2(\xi)]^{3/2}}\left(1 - \frac{3\eta^2}{2[\eta^2 + \zeta^2(\xi)]}\right). \tag{A4}$$

Here, $\zeta(\xi)$ satisfies the differential equation

$$\left(\frac{d\zeta}{d\xi}\right)^2 + \frac{1}{\sqrt{\eta^2 + \zeta^2(\xi)}} = 1, \tag{A5}$$

where $\xi =$ is chosen so that $\zeta^2(\xi)$ is even in ξ. This is the case when $\zeta^2(0) = \max(0, 1 - \eta^2)$. Also, note that in Eqs. (A3) and (A4) κ stands in for $\kappa = \bar{\kappa}/\sigma^3$.

This article is copyrighted as indicated in the article. Reuse of AIP content is subject to the terms at: http://scitation.aip.org/termsconditions. Downloaded to IP: 132.239.69.167 On: Wed, 18 Mar 2015 17:53:47

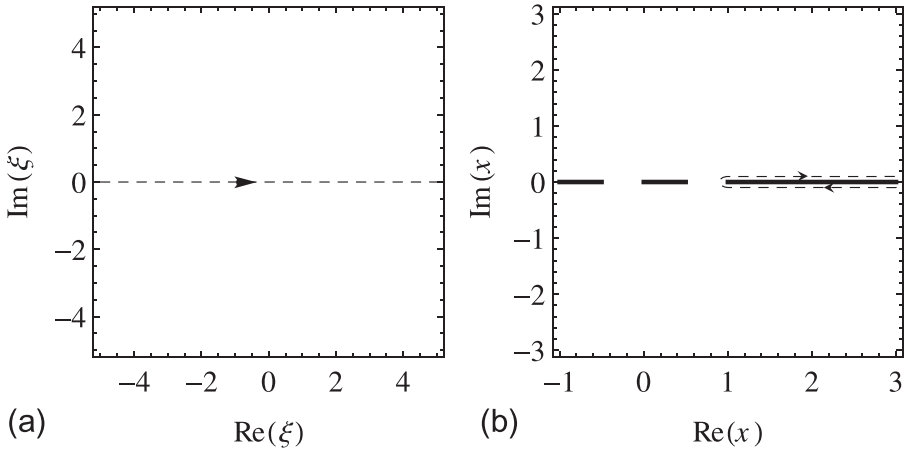

FIG. 13. Path (dashed curve) of the original contour in ξ-plane (a) and x-plane (b). Branch cuts are denoted by thick solid lines, and in this figure, $\eta = 0.5$.

For large $\bar{\kappa}$, the integrands in Eqs. (A3) and (A4) involve the product of a rapidly oscillating function and a slowly varying function, and efficient evaluation of such integrals can be effected through analytic continuation. Following the earlier work of O'Neil and Hjorth,[4] we define $x = \sqrt{\eta^2 + \zeta^2(\xi)}$, which satisfies the differential equation

$$\frac{dx}{d\xi} = \frac{i\sqrt{x-\eta}\sqrt{x+\eta}\sqrt{x-1}}{x\sqrt{-x}}, \tag{A6}$$

where $x(\xi = 0) = \max(\eta, 1)$. In the square roots of Eq. (A6), the branch cut for any function $\sqrt{w(x)}$ is taken along $\arg w(x) = 0$. The Right Hand Side of Eq. (A6) then has branch cuts for $x < -\eta$, $0 < x < \min(\eta, 1)$ and $x > \max(\eta, 1)$.

We first consider the case where $\eta < 1$, that is, where there is reflection. The case of no reflection ($\eta > 1$) follows similarly. For $\eta < 1$, the branch cuts are indicated by the thick solid lines in Fig. 13(b). As ξ moves from $-\infty$ to ∞ along the dashed contour in Fig. 13(a), $x(\xi)$ moves along the dashed contour in Fig. 13(b), reaching the turning point $x = 1$ at $\xi = 0$, i.e. $x(0) = 1$. Because $x(\xi)$ is even in ξ, the integrals in Eqs. (A3) and (A4) can be rewritten as

$$f_1(\kappa, \eta) = \int_C \frac{\exp(i\kappa\xi)d\xi}{x^3(\xi)}, \tag{A7}$$

$$f_2(\kappa, \eta) = \int_C \frac{\exp(i\kappa\xi)d\xi}{x^3(\xi)}\left[1 - \frac{\eta^2}{x^2(\xi)}\right]. \tag{A8}$$

The goal here is to analytically continue the ξ-contour so that the integrands themselves exhibit the exponentially small value of the integrands, so we push the ξ-contour toward positive imaginary values. The deformation can continue until the $x(\xi)$ contour collides with the branch cut ending at $x = \eta$ as shown in Figs. 14(a) and 14(b).

During the deformation, the turning point moves from $x = 1$ to $x = \eta$, and ξ-image of the turning point moves from $\xi = 0$ to

$$\xi = ig(\eta) = i\int_\eta^1 \frac{x^{2/3}dx}{\sqrt{1-x}\sqrt{x^2-\eta^2}}, \tag{A9}$$

where use has been made of Eq. (A6). The two points around which the x-contour loop are the images of $x = 0$ approached from opposite sides of the branch cut between $x = 0$ and $x = \eta$. From Eq. (A6), we see that the coordinates of these two points in the complex ξ-plane are $\xi = ig(\eta) \pm r(\eta)$, where

$$r(\eta) = \int_0^\eta \frac{x^{2/3}dx}{\sqrt{1-x}\sqrt{\eta^2-x^2}}. \tag{A10}$$

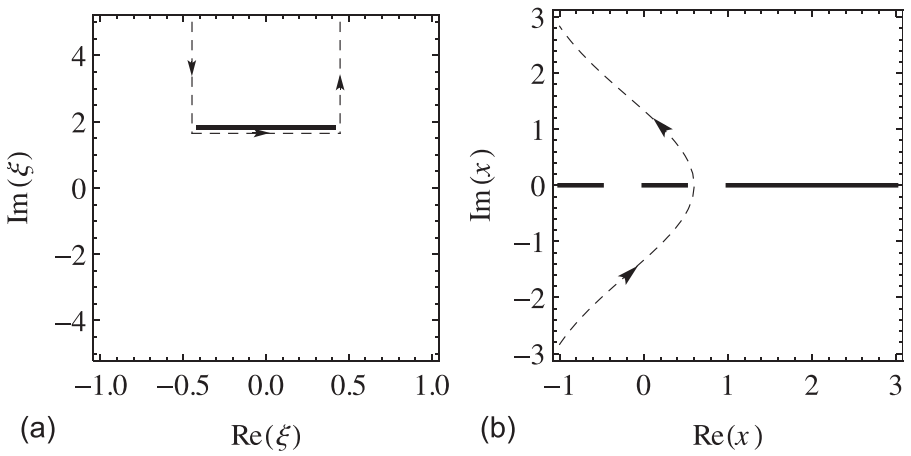

FIG. 14. Path (dashed curve) of the deformed contour in ξ-plane (a) and x-plane (b). Branch cuts are denoted by thick solid lines, and in this figure, $\eta = 0.5$.

This article is copyrighted as indicated in the article. Reuse of AIP content is subject to the terms at: http://scitation.aip.org/termsconditions. Downloaded to IP: 132.239.69.167 On: Wed, 18 Mar 2015 17:53:47

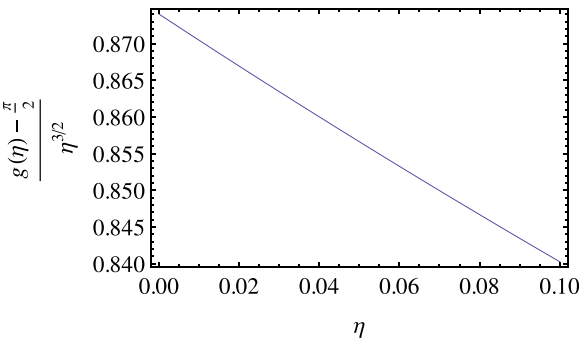

FIG. 15. Curve fitting of $g(\eta)$ against η, showing that $g(\eta) - g(0) \sim \mathcal{O}(\eta^{3/2})$.

There is a branch cut between the two points in the function $x(\xi)$.

Since the singularities of the integrands in Eqs. (A7) and (A8) involve more than just isolated poles, the integrals cannot be expressed as the sum of residues. Nevertheless, for sufficiently large κ, one can see that the integrals are of order $\exp[-g(\eta)\kappa]$, that is, one obtains the asymptotic forms $f_j(\kappa,\eta) = h_j(\kappa,\eta)\exp[-g(\eta)\kappa]$ quoted in Eqs. (20) and (21) of Sec. II. Here, the quantities $h_j(\kappa,\eta)$ are neither exponentially small nor large, and for small η are given by[4] $h_j(\kappa,\eta) \simeq 8\pi\kappa/9$.

The integrals also are evaluated by numerically carrying out the ξ-integral along the deformed contour in Fig. 14(a). Fig. 1 of Sec. II shows a comparison of the numerical and asymptotic evaluations of $f_1(\kappa,\eta=0) = f_2(\kappa,\eta=0)$.

Returning to an evaluation of integrals (A3) and (A4), we first note that $g(\eta)$ is an increasing function of η. Thus, for sufficiently large values of $\bar{\kappa}$, only small values of η contribute to the integrals, and we may use the approximation $h_j(\kappa,\eta) \simeq h_j(\kappa,0) = 8\pi\kappa/9$, or $h_j(\bar{\kappa}/\sigma^3,\eta) \simeq h_j(\kappa,0) = 8\pi\bar{\kappa}/(9\sigma^3)$. Also, for small values of η, one can see by curve fitting that $g(\eta) \simeq \pi/2 + \lambda\eta^{3/2}$, where $\lambda = 0.874$ (see Fig. 15). The integrations over η can then be carried out in Eqs. (A3) and (A4) yielding the integrals

$$\Lambda_1(\bar{\kappa}) = \left(\frac{8\pi}{9}\right)^2 \frac{\bar{\kappa}^2}{(2\bar{\kappa}\lambda)^{8/3}} \cdot \frac{2}{3}\Gamma\left(\frac{8}{3}\right)\int_0^\infty d\sigma\sigma e^{-\sigma^2/2} e^{-\pi\bar{\kappa}/\sigma^3}, \tag{A11}$$

$$\Lambda_2(\bar{\kappa}) = \left(\frac{8\pi}{9}\right)^2 \frac{\bar{\kappa}^2}{(2\bar{\kappa}\lambda)^{4/3}} \cdot \frac{2}{3}\Gamma\left(\frac{4}{3}\right)\int_0^\infty d\sigma\sigma e^{-\sigma^2/2} e^{-\pi\bar{\kappa}/\sigma^3}. \tag{A12}$$

The σ-integrals in these two equations are identical and involve the product of an exponentially decreasing function, $\exp(-\sigma^2/2)$, and an exponentially increasing function, $\exp(-\pi\bar{\kappa}/\sigma^3)$. Evaluating the integrals by the saddle point method yields the large $\bar{\kappa}$ asymptotic formulae,

TABLE I. Numerically integrated values of $\Lambda_1(\bar{\kappa})$ for different values of $\bar{\kappa}$.

$\bar{\kappa}$	$\Lambda_1(\bar{\kappa})$	$\bar{\kappa}$	$\Lambda_1(\bar{\kappa})$
5	0.222	200	5.06×10^{-8}
10	5.06×10^{-2}	300	6.92×10^{-10}
20	7.71×10^{-3}	500	1.29×10^{-11}
50	2.41×10^{-4}	700	2.89×10^{-13}
100	5.95×10^{-6}	1000	3.15×10^{-15}

TABLE II. Numerically integrated values of $\Lambda_2(\bar{\kappa})$ for different values of $\bar{\kappa}$.

$\bar{\kappa}$	$\Lambda_2(\bar{\kappa})$	$\bar{\kappa}$	$\Lambda_2(\bar{\kappa})$
0.01	3.250	20	2.837×10^{-1}
0.05	3.230	50	3.074×10^{-2}
0.1	3.201	100	2.338×10^{-3}
0.7	2.850	200	4.989×10^{-5}
2	2.419	350	1.685×10^{-6}
6	1.251	500	4.195×10^{-8}
10	7.523×10^{-1}		

$$\Lambda_1(\bar{\kappa}) = 3.10\bar{\kappa}^{-7/15} e^{-5(3\pi\bar{\kappa})^{2/5}/6}, \tag{A13}$$

$$\Lambda_2(\bar{\kappa}) = 3.87\bar{\kappa}^{13/15} e^{-5(3\pi\bar{\kappa})^{2/5}/6}. \tag{A14}$$

Numerical evaluations of $\Lambda_1(\bar{\kappa})$ and $\Lambda_2(\bar{\kappa})$ have been carried out for a series of $\bar{\kappa}$ values. At each of these values, the quantities $h_j(\bar{\kappa}/\sigma^3,\eta)$ are evaluated for an array of (σ,η) values using the analytic continuation described earlier. The integrands are peaked near some values (σ_0,η_0), and the (σ,η) integrands are evaluated by choosing (σ,η) values near the peak and smoothly interpolating the integrand between these points. The results of the integration are given for a series of $\bar{\kappa}$ values in Tables I and II. Also, Figs. 16 and 17 show a comparison of the numerical evaluations (dots) and the asymptotic formulae (solid curves).

We can compare our results with previous work. If we consider equipartition of a strongly magnetized single-species plasma, where $n = n_1$ and $n_2 = 0$, $T_{\perp 1}$ equilibrates with $T_\parallel$ following the rate equation

$$\frac{dT_{\perp 1}}{dt} = (T_\parallel - T_{\perp 1})\bar{n}_1\bar{b}^2\bar{v}_{11}I(\bar{\kappa}_{11}), \tag{A15}$$

where $I(\bar{\kappa}_{11}) = \sqrt{2\pi}\Lambda_1(\bar{\kappa}_{11})/8$ from Eq. (63). The function $I(\bar{\kappa})$ was evaluated in the work of O'Neil and Hjorth[4] and Glinsky *et al.*[3] In Fig. 18, numerical values of $I(\bar{\kappa})$ in our work are plotted as points together with values obtained by Glinsky *et al.* using Monte Carlo simulations. The different

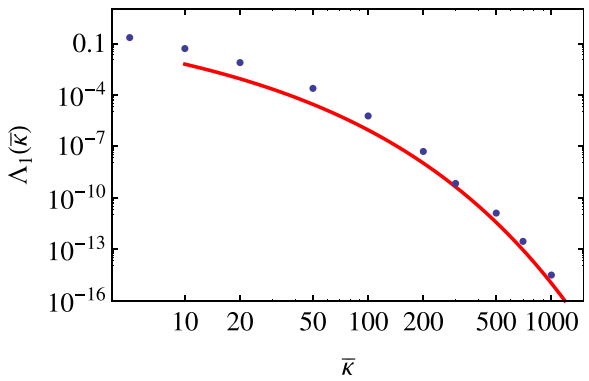

FIG. 16. Numerically integrated values of $\Lambda_1(\bar{\kappa})$ (dots) and its asymptotic graph (red line).

This article is copyrighted as indicated in the article. Reuse of AIP content is subject to the terms at: http://scitation.aip.org/termsconditions. Downloaded to IP: 132.239.69.167 On: Wed, 18 Mar 2015 17:53:47

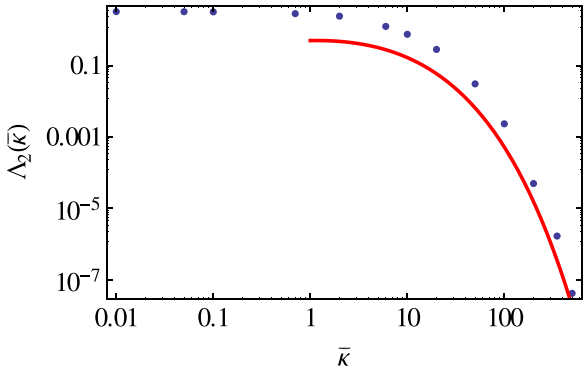

FIG. 17. Numerically integrated values of $\Lambda_2(\bar{\kappa})$ (dots) and its asymptotic graph (red line).

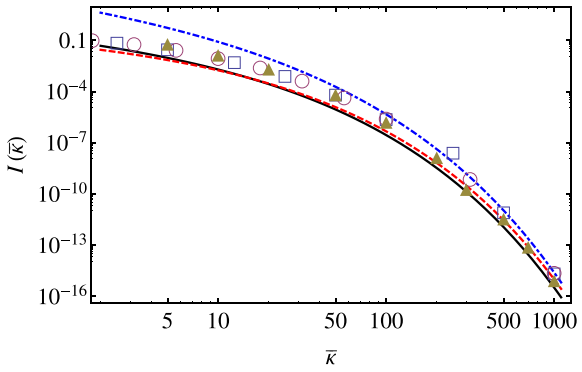

FIG. 18. Numerical values and asymptotic graphs of $I(\bar{\kappa})$. Solid triangles correspond to our calculated values. Empty circles and squares are values calculated by Glinsky *et al*. using two different sets of Monte Carlo simulations.[3] The solid line is the graph of our asymptotic expressions. The dashed and dot-dashed curves corresponds to the asymptotic expressions from O'Neil and Hjorth and Glinsky *et al*., respectively.

sets of values follow very close trends. Furthermore, in the limit of large $\bar{\kappa}$, O'Neil and Hjorth obtained an asymptotic formula for $I(\bar{\kappa})$

$$I(\bar{\kappa}) = 0.47\bar{\kappa}^{-1/5}\exp\left[-\frac{5}{6}(3\pi\bar{\kappa})^{2/5}\right], \tag{A16}$$

while the asymptotic formula from Glinsky *et al*. is

$$I(\bar{\kappa}) = (1.83\bar{\kappa}^{-7/15} + 20.9\bar{\kappa}^{-11/15} + 0.347\bar{\kappa}^{-13/15} + 87.8\bar{\kappa}^{-15/15} + 6.68\bar{\kappa}^{-17/15})\exp\left[-\frac{5}{6}(3\pi\bar{\kappa})^{2/5}\right]. \tag{A17}$$

From Eq. (A13), our version is

$$I(\bar{\kappa}) = 0.97\bar{\kappa}^{-7/15}\exp\left[-\frac{5}{6}(3\pi\bar{\kappa})^{2/5}\right]. \tag{A18}$$

Our asymptotic formula is an improved version of the work of O'Neil and Hjorth. We approximate $g(\eta)$ with $\eta^{3/2}$ as the lowest-order non-constant term, which is more accurate than η^2 in the work of O'Neil and Hjorth. However, we believe the result from Glinsky *et al*. is even better, since their work investigated the cyclotron motion in much greater detail. In the same Fig. 18, we plot the graphs of the three asymptotic expressions together with the points of numerically integrated values mentioned above. All the plotted graphs and data points show the similar exponential decrease of $I(\bar{\kappa})$ with increasing $\bar{\kappa}$.

[1]B. Beck, J. Fajans, and J. Malmberg, Phys. Rev. Lett. **68**, 317 (1992).
[2]B. Beck, J. Fajans, and J. Malmberg, Phys. Plasmas **3**, 1250 (1996).
[3]M. E. Glinsky, T. M. O'Neil, M. N. Rosenbluth, K. Tsuruta, and S. Ichimaru, Phys. Fluids B **4**, 1156 (1992).
[4]T. O'Neil and P. Hjorth, Phys. Fluids **28**, 3241 (1985).
[5]T. O'Neil, P. Hjorth, B. Beck, J. Fajans, and J. Malmberg, in "Strongly coupled plasma physics," in *Proceedings of the Yamada Conference* (Elsevier Science Publishers B.V., 1990), Vol. 24, p. 313.
[6]M. Affolter, F. Anderegg, C. Driscoll, and D. Dubin, AIP Conf. Proc. **1521**, 175 (2013).
[7]E. Sarid, F. Anderegg, and C. Driscoll, Phys. Plasmas **2**, 2895 (1995).
[8]L. Landau and E. Lifshitz, *Statistical Physics*, v. 5 (Elsevier Science, 1996).
[9]H. Goldstein, C. Poole, and J. Safko, *Classical Mechanics* (Addison-Wesley Longman, Incorporated, 2002).
[10]G. R. Smith and A. N. Kaufman, Phys. Fluids **21**, 2230 (1978).
[11]R. G. Littlejohn, J. Plasma Phys. **29**, 111 (1983).
[12]J. Taylor, Phys. Fluids **7**, 767 (1964).
[13]J. C. Butcher, J. Austr. Math. Soc. **4**, 179 (1964).
[14]D. H. Dubin and T. O'Neil, Rev. Mod. Phys. **71**, 87 (1999).
[15]S. Ichimaru, *Basic Principles of Plasma Physics: A Statistical Approach*, Frontiers in Physics (Benjamin, 1973).
[16]D. J. Evans and G. Morriss, *Statistical Mechanics of Nonequilibrium Liquids* (Cambridge University Press, 2008).
[17]F. Anderegg, X.-P. Huang, E. Sarid, and C. Driscoll, Rev. Sci. Instrum. **68**, 2367 (1997).
[18]D. H. Dubin and T. O'Neil, Phys. Fluids **29**, 11 (1986).
[19]D. Larson, J. Bergquist, J. Bollinger, W. M. Itano, and D. Wineland, Phys. Rev. Lett. **57**, 70 (1986).
[20]T. M. O'Neil, Phys. Fluids **24**, 1447 (1981).
[21]T. G. Northrop, *The Adiabatic Motion of Charged Particles* (Interscience Publishers, New York, 1963), Vol. 21.

This article is copyrighted as indicated in the article. Reuse of AIP content is subject to the terms at: http://scitation.aip.org/termsconditions. Downloaded to IP: 132.239.69.167 On: Wed, 18 Mar 2015 17:53:47